ALTA SCUOLA POLITECNICA

POLITECNICO DI MILANO | POLITECNICO DI TORINO

MULTIDISCIPLINARY PROJECT
FINAL REPORT

REGIM

Design of a regenerative damper for agricultural machines

www.asp-poli.it

POLITECNICO DI MILANO
Piazza Leonardo da Vinci, 32
20133 Milano
info-mi@asp-poli.it

POLITECNICO DI TORINO
Corso Duca degli Abruzzi, 24
10129 Torino
asp@polito.it

Stefano Cerutti, Electronic Engineering, Politecnico di Torino

Omar Kahol, Aeronautical Engineering, Politecnico di Milano

Lorenzo Mai, Engineering Physics, Politecnico di Milano

Andrea Proietti, Mechatronic Engineering, Politecnico di Torino

Duc Tan Tran, Electronic Engineering, Politecnico di Torino

Francesca Stobbione, Industrial Production and Innovation Technology Engineering, Politecnico di Torino

Principal Academic Tutor
Giovanni Maizza, Department of Applied Science and Technology, Politecnico di TO

Other Academic Tutors
Luigi Piegari, Department of Electronics, Information and Bioengineering, Politecnico di MI
Umid Jamolov, Department of Applied Science and Technology, Politecnico di TO

www.asp-poli.it

POLITECNICO DI MILANO
Piazza Leonardo da Vinci, 32
20133 Milano
info-mi@asp-poli.it

POLITECNICO DI TORINO
Corso Duca degli Abruzzi, 24
10129 Torino
asp@polito.it

List of Symbols

Geometry Symbols

μ_0	Absolute magnetic permeability
μ_r	Relative magnetic permeability of the material
τ	Pole pitch
$\mathbf{A}$	Magnetic vector potential
$\mathbf{B}$	Magnetic induction field
$\mathbf{B}_s$	Saturation magnetic induction field
$\mathbf{E}$	Electric field
$\mathbf{H}$	Magnetic field
$\mathbf{H}_c$	Coercive field
$\mathbf{J}$	Current density
C_s	Residual damping coefficient (quarter-car model)
F_D	Damping force (linear motor)
G_d	Power Spectral Density
h	Road profile displacement
k_f	Force constant (linear machine)
K_s	Spring constant (quarter-car model)
n	Spacial frequency
p	Number of pole pairs (rotary motor)
Z_m	Mechanical impedance

Electrical Quantities Symbols

Φ	Peak magnetic flux density
τ_{RL}	Time constant of the coils
B_{ref}	Reference damping coefficient
E_{abc}	Phase electromotive force
I_{dq}	d/q axis current
I_{max}	Current limit
$I_{ref,dq}$	d/q reference axis current
K_i	Integral coefficient (PI controllers)
K_p	Proportional coefficient (PI controllers)
L_s	Stator coil inductance
L_d	Direct-axis synchronous inductance
L_q	Quadrature-axis synchronous inductance
R_{eq}	Equivalent resistance "seen" at the coils terminals
R_s	Stator coil resistance
$T_{em,ref}$	Reference electromagnetic thrust (force)
T_{sw}	Switching period of the power converter
U	Instantaneous linear velocity
V_{max}	Voltage limit

Executive Summary

Agriculture has been characterized by two main innovation revolutions. The first one is associated to mechanization, through the introduction of agricultural machinery in the last decades of the XIX century. The second turning point consisted in the introduction in 1908 of the ammonia synthesis made by Haber, which set the basis for artificial fertilizers, supporting around 27% of the world population within a century [1]. In the XXI century, sustainability and optimization of resources are the new areas of innovation within the agricultural sector where the new revolution could begin. Within the current socio-economical context, which requires all companies to invest and research in sustainable development, the agricultural sector needs innovation to assure increasing efficiency with the current available land and to reduce the amount of CO_2 gas released in the atmosphere. This new third wave of innovation is predicted by the Food and Agricultural Organization of the UN (FAO) to "decrease the environmental footprint of agriculture [...] and reduce poverty and achieve food security while improving people's livelihoods" [2]. The agricultural field appears to be ready to accept substantial innovation in terms of sustainability and green technologies; yet, a lot of effort must be put to optimize and increase the consumption efficiency of agricultural machinery and to move towards a more pervasive electrification. REGIM is part of a bigger initiative driven by Frandent Group, an Italian company specialized in the production of agricultural machines and in particular power harrows, tedder spreaders and rotary rakes. The company promotes the continuous improvement of its agricultural machines through equipment that requires lower energy consumption and increases productivity.
REGIM aims to support the development of Frandent's innovative product through the design of an optimized *Regenerative Damper*, a damping system that harvests part of the kinetic energy from vibrations, which is otherwise dissipated as heat by conventional dampers, making it available for different purposes as electrical energy. The recovered energy will be used to power some of the active components of the agricultural machine, promoting electrification culture of it. The integration of a regenerative damper on agricultural machinery supports the innovation wave of sustainable mechanization and electrification.

REGIM has developed, with the help of multi-physics computer simulations and laboratory testing, an optimized design of a regenerative direct current (DC) damper technology that could substitute traditional dampers installed on the agricultural attachments chassis, which are most affected by vibrations. The design included a complete geometry definition of the regenerative DC damper and a control system to efficiently extract and convert electrical energy from the device. The prototype was designed considering the dimension and physical external requirements of a current device installed on the agricultural attachments developed by Frandent, and will, therefore, be suited to replace the conventional dampers. This way, he regenerative damper will be applied to already existing agricultural attachments to improve energy and fuel management, while fulfilling the existing aims of dissipating vibration and maintaining the structure stable.

The developed prototype consists of a moving part endowed with permanent magnets, and a fixed part with three-phase coils. The electromagnetic induction generates electromotive forces across the coils terminals when the mover oscillates. A microcontroller-based control was designed to harvest power instantaneously from the regenerator, to charge a 48 V battery. This is the typical starter battery of agricultural tractors. The complete system was simulated under typical mechanical excitation and will be experimentally tested on a test-rig. The design procedure considered the geometry configuration and control which maximise the harvested power. The simulation results showed that, from typical displacement excitation coming from the agricultural soil irregularities, few tens of *watts* can be extracted (eg: 14 W from a 1 cm, 8 Hz oscillation).

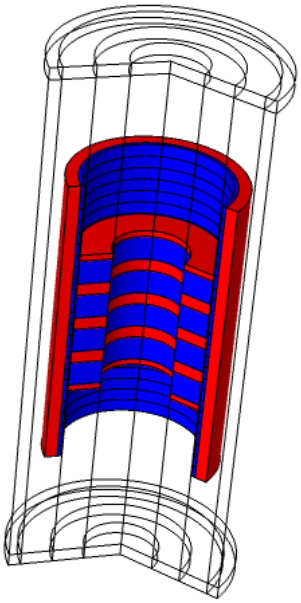

(a) 3D model of the designed regenerator.

(b) Regenerator prototype and displacement sensor mounted on the test-rig.

The designed regenerative DC damper will be integrated into an existing agricultural device, and subsequently productionised and installed within the production line of the agricultural attachments.

Future developments include studies on the utilization of the harvested energy and the connection of the battery with the active parts of the attachments will be developed by Frandent and remained out of scope for the project.

REGIM design could create a stepping stone for the sustainable mechanization of agricultural attachments. Moreover, it allowed Frandent to further support the electrification culture and optimize its products. The project results could impact the whole environment of stakeholders involved within the agricultural and food production cycle, with a more sustainable and cost efficient food harvesting process that will benefit the inhabitants of the future. In addition, the project supports the global effort of the Sustainable Development Goals by fostering the Goals of Zero Hunger (2), Affordable and Clean Energy (7) and Responsible Consumption and Production (12).

Contents

Chapter 1

Introduction

1.1 Problem statement

The demand for clean energy has been constantly increasing over the past years, and the struggle to contrast climate change requires countries to keep pushing towards the green transition. In a situation in which the impacts of climate change are already being experienced around the world, the COVID-19 pandemic further delayed the transition to greener economies.

The 2022 Sustainable Development Goals report [3] indicates that, while the economic slowdown and the lockdown induced by the pandemic helped to a temporary reduction of CO_2 emissions, the emissions related to energy production increased by 6% in 2021, with the rebound in the demand for oil, coal and natural gas. To limit the negative impacts of global warming, the current target consists in the reduction by 45% of global CO_2 emissions, compared to the levels of 2010, while experts project an increase by almost 14% during the rest of the decade. In order to mitigate the effects that climate change will bring about, the target is to limit the increase in the average temperature of the globe to well below 2 °C with respect to pre-industrial revolution period, aiming at a maximum increase of 1.5 °C. To achieve this goal, it is necessary to transition to a "greener, more inclusive and just economy" by adopting low-carbon pathways in the way we produce resources, since it is the way in which we produce and consume resources that will determine the overstepping of planetary boundaries.

In addition to reducing the impact of CO_2 emissions, part of the SDGs' mission consists in "ensuring access to affordable, reliable, sustainable and modern energy for all", as stated in the SDG 7 ("Affordable and clean energy"). At the core of this goal are two topics: to increase share of energy produced by *Renewable Energy Sources* (RES) and to improve the efficiency of the overall energy supply chain. Linked to both topics is the adoption of electricity as the main carrier of energy, making electrification of various sectors a priority in order to achieve SDG 7. Nevertheless, albeit the improvement in the use of RES and increased energy efficiency, the current progress is not fast enough to meet the expected results by the deadline of 2030. Moreover the situation risen due to the war in Ukraine has contributed to increase global energy prices and to mine the energy security of several European countries. As a response, some of them aim to expedite the adoption of more RES and increase investments both in RES efficiency and in the overall efficiency of the grid, while other countries plan a resurgence of the use of coal, undermining the green transition for all.

Thanks to technological innovation, several new opportunities arise to both generate energy with higher efficiency and also optimize its use, either by reducing the amount of energy required for a given task through new and better devices or by recovering some of the unexploited energy which would otherwise be wasted. Indeed, a lot of research has been carried out during the past decades in the field of *Energy Harvesting*. In this regard, *Regenerative Shock Absorber* systems are being studied and introduced in various fields as a way to increase the efficiency of the energy system through harvesting of energy from mechanical vibrations. The harvested energy can be stored in batteries for later use, extend the mileage of vehicles, help saving fuel and electrical energy, achieving a reduction in the Greenhouse Gases (GHG) emission [4].

Fuel energy consumed to drive the wheels has been shown to account for up to 22.5% of the total fuel energy utilized [5]. At the same time, it is estimated that only up to 16% of the fuel energy is exploited to actually drive vehicles, i.e. to overcome the resistance from road friction and air drag [6], and that vehicle suspensions have substantial influence on the fuel efficiency. During the past decades, energy recovery from vehicles' braking systems has been successfully commercialized in hybrid vehicles. Beside these, regenerative shock absorbers emerge as a promising solution for regenerative vehicle suspensions, which have the advantage of continuous energy recovery [7]. Their goal is to convert vibrational movements of the machine into useful electrical energy that can power on-board equipment immediately or be reserved in a battery for later use. In either case, the mileage of the vehicle is extended, saving fuel, and reducing the emission of greenhouse gases. Through modeling and road tests, in [7] an average $100\,\mathrm{W} - 400\,\mathrm{W}$ of energy harvesting potential was estimated in the suspension of typical passenger vehicles traveling at 60 miles per hours on standard and regular roads. Especially for heavier vehicles driving over rough and uneven surfaces the percentage of the dissipated fuel is expected to be considerably higher, with more energy available for recovery through energy harvesting.

1.2 Objectives of the project

The aim at the core of the REGIM project is to design and develop a regenerative shock absorber that is able to harvest the vibrational energy of agricultural machines when operating, and transform it into useful electrical energy. Current traditional systems are based on mechanical friction and dissipate as heat the mechanical energy subtracted from the vibrations. The innovation promoted by REGIM pursues the goal of finding alternative exploitation of otherwise wasted energy, in perspective of a more responsible consumption of resources.

There are currently several applications of this technology in the automotive industry, such as regenerative suspension systems for electric cars; however, REGIM is proud to be the first project to bring the idea into the agricultural machinery sector. *Frandent Group*, an end-user leader in the construction of agriculture machines and appliances, will benefit from this cutting edge technology. The agricultural field looks ready to accept substantial innovation in terms of sustainability and green-technology. Electrification is nowadays a key trend in many sectors, including agriculture; however, a more pervasive electrification still requires lot of effort in the optimization and efficiency increase of agricultural machinery.

The ultimate goals are the promotion of the electrification culture and the fostering of the Sustainable Development Goals 2,7 &12. These will be achieved applying a regenerative DC damper technology in the parts of the vehicles that are most affected by vibrations. The main constrains that limited the diffusion of other initiatives and might slow down the development of our device range from the high cost of the most effective solutions to low maintainability and reliability. REGIM's device will replace the conventional dampers already installed in all machines, fulfilling the existing damping goal while also providing the additional benefit of energy harvesting. The regenerative damper will be applied to agricultural tractors (both hybrid and traditional) to improve energy and fuel management (thus increasing the overall efficiency), or to attachments to drive self-sufficiency. In the latter case our devices could also be exploited to extract energy from otherwise passive attachments, contributing to create a positive energy balance.

1.3 Impact potential of the project

The project covers several important areas in the agricultural sector that present unexploited opportunities for an increased sustainability. The main issues to be addressed and the measures to be adopted are described by the Sustainable Development Goals (SDGs) 2, 7 and 12. The regenerative damper proposed in this project is expected to bring a positive impact onto these 3 crucial goals.

Goal 2: ***End hunger, achieve food security and improved nutrition and promote sustainable agriculture***

The topic of sustainable agriculture is quite controversial, since, on the one hand, the industrial approach to food production, with its reliance on monoculture, mechanization, use of chemical pesticides and fertilizers, has a negative social and ecological impact; on the other hand, the complete rejection of this model would result in lower crop yields and higher land use. With the increase in global population, sitting at around 8 billions at the present and projected towards 10 billions by 2050 [1], a reduction in the productivity will mean inevitable food shortages for vast portions of the population. A hybrid approach will most likely be required, trending towards the electrification of agriculture, the requalification of hilly terrains, and the reduction of emissions and of the use of artificial fertilizers. The regenerative damper proposed in this project aims at reducing the impact of the modern system of agriculture, while acknowledging the importance of mechanization.

Goal 7: ***Ensure access to affordable, reliable, sustainable and modern energy for all***

The term *energy* is often misunderstood and used interchangeably with the term electricity, while the latter is only one of the possible forms in which energy can be stored or exchanged. Nevertheless, electricity constitutes the most efficient and green carrier of energy available and the electricity sector records the highest share of RES in total production and consumption (26.2% in 2019[2]) and is propelling most of the growth in the use of renewable energy. The heating and transport sector, however, is still bound to a fossil fuel-based approach and experiences a

[1] *UN World Population Prospects 2019*, available at https://www.un.org/development/desa/en/news/population/world-population-prospects-2019.html

[2] *IEA Global Energy Review 2019*, available at https://www.iea.org/reports/global-energy-review-2019

lower exploitation of renewable sources. REGIM's project aims at tackling two main issues in this regard:

1. increase the efficiency of the consumption of energy, either by reducing the fuel consumption of combustion engines, by reducing the amount of energy required to recharge the battery or to power external appliances; or by prolonging the autonomy of electric vehicles;

2. promote the electrification of agriculture, which constitutes a laggard sector in this regard with respect to other fields, and take a further step towards what is named *Agriculture 4.0*.

Goal 12: *Ensure sustainable consumption and production patterns*

In 2009, Rockström introduced the concept of *planetary boundaries* delimiting the safe operating space for humanity to maintain the stable situation of planet earth that has allowed the rise of civilization [8]. Responsible production and consumption of key resources such as food, clean water, raw materials, fossil fuels *etc.*, covers a key role among the SDGs, as it determines in large part the overstepping of such boundaries. Several actions surely need to be taken in order to limit the resource footprint of food in the distribution and consumption phases, indeed "the proportion of food lost globally after harvest on farm, transport, storage, wholesale, and processing levels, is estimated at 13.3% in 2020[3]". Nevertheless, a further action which can be taken to reduce the overall footprint of food production consists in limiting CO_2 emissions and reducing the consumption of fuel exploited to produce it. This last, crucial point is specifically tackled by this project.

1.4 Methods and tools

Due to its intrinsic multidisciplinarity, the project development required the combination of parallel and joint working approaches. Since the project is mainly articulated into two broad objectives (design of the physical generator, and design of the electronic interface with the battery to be recharged), the team was split from the beginning into two subgroups: *Multyphysics* and *Power Electronics*. The two subgroups, beside working in parallel on partial goals, acquired specific knowledge and exploited specific competences in the use of pieces of software and design approaches.

The Multiphysics group, through an iterative approach, aimed to optimize a pre-existing and general-purpose permanent-magnet tubular generator to make it compliant with application-specific space constraints and output power specifications. The reference tool exploited for these objectives was *Comsol Multiphysics* 5.6 and 6.0[4], a simulation environment optimized for the integration of multiple physics dimensions (electromagnetic, mechanic, thermal modelling, *etc.*). The tool provided support through the entire design process, from the preliminary selection of the geometry and materials, to the parametric optimization of the generator properties.

The Power Electronics group, on the other hand, aimed to design the power electronics interface between the generator and the load (a 48 V lead-acid rechargeable battery), both in terms of conversion-chain topology and control. A preliminary state of the art review allowed to acquire

[3] *SDG Progress Report 2022*, available at https://sustainabledevelopment.un.org/content/documents/29858SG_SDG_Progress_Report_2022.pdf

[4] https://www.comsol.com/comsol-multiphysics

skills in the generator electrical modelling and to define the state of the art of possible control techniques. Plexim *PLECS* 4.6.4[5] and Mathworks *Matlab/Simulink* 2022*a*[6] were exploited for preliminary simulations on device-independent permanent-magnet motors control. The successive definition of the hardware for the prototype laboratory testing required, instead, to use target-specific design environments, such as Texas Instruments *Code Composer Studio* 11.2.0[7], Texas Instruments *ControlSUITE* 3.4.9 [8], and a device-specific package for *Matlab/Simulink*, *Embedded Coder Support Package for TI C2000 Processors*[9].

Beside the parallel working goals, a joint approach was fundamental to establish shared and broader objectives, and to support technical design choices. Critical issues needing a coordinated effort were the following:

- definition of geometric constraints, output power target and maximum mechanical excitation of the generator;
- extraction of an equivalent-circuit model for control purposes from the physics-based model developed on *Comsol Multiphysics*. This passage was crucial to establish a coherent link between the physical and the electrical domains of the regenerator model;
- experimental setup design and laboratory testing.

[5] https://www.plexim.com/products/plecs

[6] https://it.mathworks.com/products/matlab.html

[7] https://www.ti.com/tool/CCSTUDIO

[8] https://www.ti.com/tool/CONTROLSUITE

[9] https://it.mathworks.com/hardware-support/ti-c2000-embedded-coder.html

1.5 Organization of the report

The present report aims to provide the necessary economical and technical backgrounds in which the project was involved, and to present the final results obtained with the proposed designed solution. This work is organized as follows.

Chap.2 outlines the stakeholders' environment in which the project operated. The analysis present the trends and initiative that are driving the environment, leading to the classification of the main stakeholders involved. Specifically, the chapter highlights the links between the primary stakeholders' needs and requirements within the Frandent reality. In conclusion, the requirements are translated into REGIM design's specifications.

Chap.3 introduces tasks and operating principle of a damper, and frames the current state of the art of dampers. In order to justify the choices made in the design flow, the current damper technologies are classified according to the following criteria:

- the energy harvesting mechanism;
- the energy conversion chain configuration;
- how the damping coefficient is determined and/or controlled;
- geometry of the damper;
- the materials and arrangement of permanent magnets;
- the power electronic converter and its relative control.

Chap.4 presents the design flow from both the physical modelling and control design perspectives. At the beginning of the chapter, a possible modelling approach for road mechanical excitations is outlined, to provide the theoretical background behind the target mechanical system. More technical details on the control design flow can be found in Appendix Appendix A.

Chap.5 reports meaningful simulated and experimental results, to validate the physical and control design processes. Both *Comsol Multyphysics* and *Matlab/Simulink* simulations are reported, including *Processor-in-the-loop* (PIL) simulations. At the end of the chapter, the experimental setup and procedure foreseen in this project are described. Actually, due to prototype manufacturing defects, the complete experimental testing phase could not be carried out: this report only presents partial results on the characterization of the prototype coils.

Further testing is under way to evaluate the overall performances and validate the design. The team will be working on such experiments also beyond the presentation deadline, in look also for a possible scientific publication. The remaining tests and expected outcomes will be discussed in the *Conclusion and Future Developments* chapter.

Chapter 2

Stakeholders' analysis

The aim of REGIM is the development of the optimal geometry of a regenerative damper, that will be later tested and developed with production equipments integrated with Frandent product lines. The REGIM project therefore is an integral part of the R&D phase of the damper components for Frandent products. The project is not intended to create a final product itself. Nevertheless, REGIM impacts and create value to the whole environment connected to Frandent products.

We can split requirements and stakeholders looking at long and shorts term scenarios. While REGIM is actively involved in fulfilling the requirements and needs of the short time strategy, its requirements must not contradict long terms needs.

2.1 Frandent background

Frandent Group SRL, founded in 1977 in Osasco (TO), has specialized in the production of agricultural machinery and in particular of rotary harrows, tedders and rotary rakes. In 2006, with the opening of the new headquarters, Frandent introduced significant innovations concerning the production process and sustainable energy management. In July 2021, the BUREL Group has acquired the majority of Frandent, this company devotes 5% of its turnover to research [9] and has a dedicated research and design center, which will further support the company's mission regarding innovation. Frandent and its parent group work in a international scale, with presence to sector innovation events such as the International Agricultural and Gardening Machinery Exhibition. The company horizon of clients and stakeholders is not limited to the national borders.

The company has great interest in sustainable transformation, as also reflected in the values and sustainable transformation applied to infrastructure and processes. The key paradigms of Frandent's work are efficiency and the elimination of waste and the approach to renewable energy sources.

The first point is applied with the incentive of the Lean Production System with a production organization method based on just-in-time and the elimination of all types of waste. The second is articulated in a strong push towards R&D and on waste reduction policies. The use of renewable sources is an additional goal towards the independence from harmful sources to the environment. The company is already a leader of different breakthrough innovations, with 4 patents granted in the field of agricultural machines.

Therefore, REGIM effort supports the long term objective of both needs of Frandent with the overall interest directed to the integration of regenerative dampers in agriculture machinery and in driving the agricultural sector towards more sustainable paths.

The idea of a regenerative dampers for agricultural purposes was developed from the collaboration between the Polytechnic of Turin and Frandent. The collaboration between the two entities already produced an innovative solution [10]. Moreover, studies have been carried out to analyse the potential of an agreement among Government, Industry, University, Research and

Promotion for cutting-edge innovation products. Especially for the design side of new technologies, this type of agreement has been found essential from China agriculture and agricultural mechanization technology innovation, that have not yet been established. [11] The externalization of the technology definition to a research group improves the expansion of a research detached from the company development view. While there is the risk of not prioritizing the same parameters, if a correct alignment of the entities is carried out, the independence of the two will create a prolific collaboration that will be integrated in the production phase with the company framework.

2.2 Industry trends analysis

The user requirements of the environment of agriculture machines and shock absorbers are influenced by the industry trends in this sector.

When it comes to agriculture industry, the reduction of the ecological footprint of the harvesting process and the whole production chain is under scrutiny. Both regulatory bodies and companies are trying to measure the utilities consumption impact and what are the solutions to optimize it. The utilities footprint of agricultural machines has been studied in recent years [12] and resulted to have a greater food print in term of water and energy demand than tractors. In addition, agricultural machine Power Take-Off (PTO) elements, alimented through electricity by an external battery, have been compared to standard machine operated via petrol. This comparison has shown that electrical PTOs could, among other benefit, decrease fuel consumption between 30 to 33% [13].

Agricultural machines are indispensable for an economic positive productivity, therefore defining when agriculture is a source of poverty or a part of the economy. Nevertheless, their sustainable impact contribute significantly to the whole value chain. Therefore, the Food and Agricultural Organization of the United Nations promotes sustainable agricultural mechanization as a mean to increase productivity and efficiency with scarse resources [14]. In this perspective, mechanization should help producers to both decrease the environmental impact and improve profitability, thus enhancing food security. Sustainable mechanization is addressed by FAO as a mean to reduce poverty and improve people's wellness.

The regenerative dampers' market is growing both technologically and economically thanks to funds for green technologies starting from public and private initiatives, the establishment of sustainable industries and Governments incentives and policy making. The automotive shock absorbers market is thusly predicted to expand at over 5% CAGR through 2031 [15]. As a consequence, the regenerative dampers' solutions and market will benefit, as well.

In this regard the future trends of the regenerative shock absorber would be high power to weight ratio, better mechanical-electrical conversion efficiency and higher compatibility with the vehicle [4].

2.3 Stakeholders' environment

2.3.1 Main stakeholders

Frandent mission, stating "we know the land our customers work and we satisfy their needs by providing the best solutions.", introduces the agricultural machines owner and their users as the two main groups of stakeholders.

Investors are pivotal to make electromagnetic regenerative dampers commercially viable; in fact, substantial investments would be required to develop a proper manufacturing and distribution network, capable of competing in a market dominated by conventional dampers. Regarding the latter, the presence of an already established and cost-effective technology could make the entrance of our product on the market difficult, and it is likely it would take years before it becomes widespread enough to generate profit. These factors could make investors reluctant and limit their support. However, they could be encouraged to invest in the product by the fact that the technology already exists and only needs to be adapted to a different field, making investments safer and reducing the amount of funds to be spent solely on research and development.

The regenerative market environment efforts is characterized by specific stakeholders for each application scenario of Frandent. In the Italian scenario, the Federazione Nazionale Costruzione Macchine per l'agricoltura (FederUnacoma) is one of the main promoters of innovation, with specific associations for each sector. Among these, ASSOMAO, the Association of Italian manufacturers of implements, to which Frandent belong and is active member. FederUnacoma actively promotes the investments of companies on new technology throughout services of internationalization, patent and regulatory support, events and other initiatives.

The internationalization effort of the group with the recent acquisition from BUREL could lead to an entrance in the stakeholders environment of European and worldwide associations. The main groups of interest for the project are Axema, the French union of agriculture machines producers and AEA, for the British expansion of manufacturers and producers of machinery. Moreover, the long term strategy might include the expansion of the technology of regenerative dampers to additional agricultural applications, therefore initiatives developing electric tractors like the GridCON project or Monarch tractors (USA) might look into the product to expand its adoption range. In the graph below, the stakeholders discussed are presented based on their interest level in REGIM and ability to influence the final product that will be developed by Frandent. The categorization is needed to prioritize the requirements.

The innovators and early adopters of regenerative dampers solutions are industries producing agricultural machines that share the following characteristics:

1. focus on green technologies (e.g. electric tractors);
2. small industries/startups;
3. eagerness to improve their current machines.

2.3.2 Analysis of stakeholders' needs

The innovators and early adopters of technology, in connection with the stakeholders of Frandent, create the environment where the project deliverables are extracted. On the other side of the value chain are the two groups of customers, both direct and indirect. The first one consists of the owners of agricultural machines, while the second one is constituted by the users of the equipment itself. While the two groups may coincide in the same physical person, the requirements and needs are distinct and in part incongruous. By analyzing the two customers, through focus groups and indirect sources, the needs related to long term technical and economical requirements have been driven.

The lock-in effect created by the current paradigm stems from the changes that the standard design of many agricultural machines would be required to undergo to integrate REGIM's product. Even though the design of the agricultural machines would not be revolutionary, the

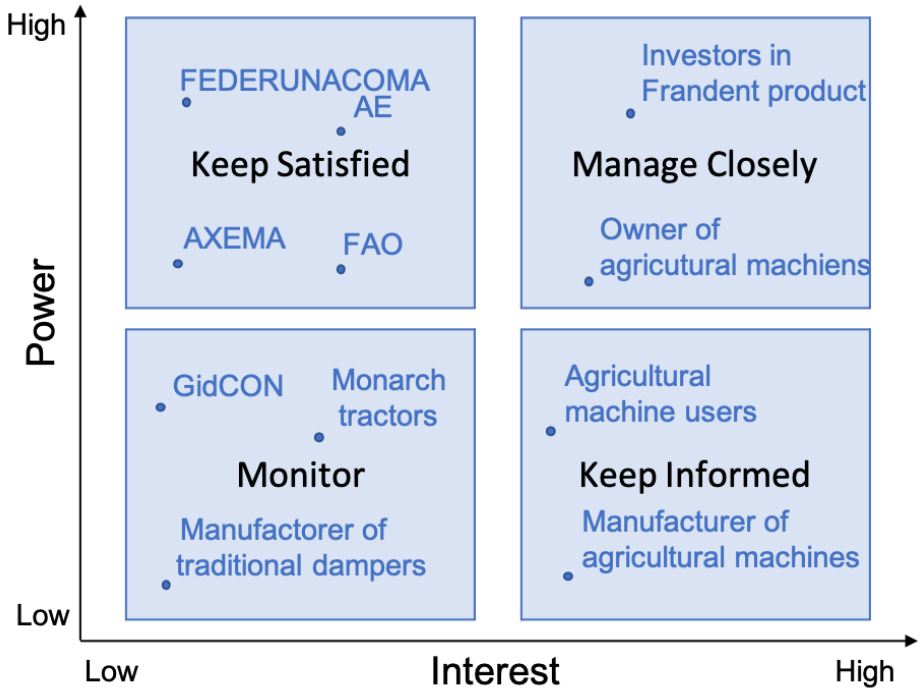

Figure 2.1: Categorization of stakeholders based on power-interest dynamics.

physical dimensions between electromagnetic regenerative and conventional dampers ought to be taken into account: the standard dimensions of a damper used in Frandent products set the dimension constraints for the new product. Nevertheless, the paths for the cables connecting the dampers to the battery and a space for the electronic components need to be allocated: therefore, further analysis must be carried out to reduce costs related to the regenerative dampers integration on agricultural machines. This need, strictly linked to the economic viability of the complete system, can be classified among the long term needs.

Additionally, tests must be performed in order to assess the functionality and safety of the modified design. In particular, the casing of the dampers needs to be tested thoroughly in a way that properly reflects the working conditions of agricultural machines, since infiltration may result in damage to the electrical network of the whole machine. The lock-in may be caused by the aforementioned technical challenges and the costs related to it, as well as by the dominance of conventional dampers on the market.

Evaluating the characteristics of agricultural machines, the main needs to be tackled are:

1. fossil fuel consumption: most agricultural machines are fueled by diesel and a third of energy consumed in agriculture is due to machinery [16]. Fuel costs have a huge impact on the economic needs;

2. ride comfort of operators: machine operators spend a great amount of time on the farmland. It is necessary for the machine to attenuate vibrations, so that the operators would have more comfortable drives;

3. loudness: conventional machines are noisy when operating. The damping of vibrations could reduce the noise to some extent.

On the damper side, the following needs must be tackled:

1. resistance to harsh environments: the damper should be able to survive in the agricultural environment. This means that it must be resistant to water, humidity, dirt and chemical products; moreover, it should be able to resist to pressure washing;

2. technical requirements: the system must be compatible with the requirements in terms of size and weight, each subsystem must be easily accessible and repairable. It is also required to ensure reliable over time.

Technical	Noise reduction	Noise impact level below limits
Technical	Reduce consumption of CO2	Maximization efficiency of regenerative side
	Increase productivity	
	Increase autonomy	
Technical	Reliability	Waterproof, dirtproof, pressure washable and resistant to chemicals device
Technical	Confort	Maximize damping coefficient
Technical	Ease on repair	Ensure ease of access and swap of components
		Create a maintenance package to offer repair through attachment producers
		Modular design and assembly
Technical	Specification standards	Standardized sub- components
		Compliant external geometry to exsisting measure
Regulatory	Standard Regulation compliance	Implement all applicable standards or
		Mapping of new compliance definition
Regulatory	Safety assurance	Perform extensive testing in harsh conditions
		Audits and maintenance plan
Business	Maintain the already-established customer spectrum	Guarantee and communicate the fulfilment of all previous standards
Business	Ensure market ownership	Develop patented solutions
		Work with patent attached relationships
Business	Attract institutions incentives and public attention	Impact of fuel consumption reduction through energy recovery measurement
Business	Reduce costs of production	Balance performance to cost of piece to maximize ratio of cost per unit of product produced
Human based	Respect of the environment	Use of sustainable and eco-friendly materials and chemicals
		Limit the use of hazardous chemicals
		Decrease waste in production line

Table 2.1: Frandent's Needs and Requirements.

To summarize, an agricultural machine endowed with a regenerative damping system is expected to present the following characteristics:

- provide ride comfort for the user;
- maintain or enhance driving safety;

- actuate efficient power recovery;
- geometry specification conformance with existing pieces;
- reliability and maintenance easiness.

2.4 REGIM User's Requirements

In order to derive the specification of the project, the short term needs of Frandent need to be identified and converted to requirements for REGIM. The process used to define the final requirements started, as presented above, within the analysis of the needs of the stakeholders of Frandent. This analysis produced the requirements for Frandent itself. Frandent stakeholder environment includes both long and short term requirements.

Parts of technical functionalities and regulatory elements need to be considered on the short term strategy and constitute the main Frandent needs, which REGIM needs to address. On the other hand, socio-economical aspects, not connected with the efficiency of the energy harvesting system, remains long term requirements connected to the product ionization and the inclusion of regenerative dampers within agricultural machine, and thusly out of scope for REGIM.

Frandent long term strategy require the unlock of the technology needed for the partial electrification of its devices. Therefore, REGIM final user requirement is the development of new optimized geometry for regenerative dampers. This will be the enabler to the integration to the agricultural machine market of regenerative dampers.

While the durability of the damper is not a feature that needs to be applied in the short term, the other technical components are fundamental for the short term strategy and REGIM's aim. On the feasibility side, both damping coefficient and recovery efficiency are develop in the product design. Production costs optimization are out of scope, while on the contrary, availability of standard components remains a requirement in the geometry optimization, with a latter priority. Lastly, the main lock-in of the device is the conformance with the current dimension and external geometry configuration of the regenerative dampers.

The S curve of development of the technology and the market provide an important basis to transform the needs in requirements.

Regarding REGIM's output, the regenerative damper is the system, while the supra-system interaction with it is the agricultural machine. At a lower scale, the individual components are defined as sub-systems. Each subsystem of regenerative dampers (starting from material to produce parts to the actual coils and magnets) has a validated and well established technology. The overall technology is still at an early stage because the correct and efficient integration of these submodules is still far from being ready for the market. This can explain the fact that there are still many different solutions and a dominant design is yet to emerge. Our solution will thusly be an entrant in the market and will try to establish a dominant design in the agricultural field.

No direct competitor can be identified since no other company or entity is involved in our target industry (agricultural machines). Groups like Audi and ZF are developing technology for different fields but the production line of Frandent requires specific technical aspects that are not developed by the companies. Moreover, the large scale of business in which the groups operate would not be scalable economically to a still contained application field.

REGIM product damps relative motion of a chassis with respect to the ground and converts the relative motion into electrical energy exploited to charge a battery. One of the main technical parameters to define the performance of a damper is the capability to effectively provide

oscillation damping on the vibrating mechanical structure: this performance is quantified in the parameter *damping coefficient*. Electromagnetic regenerative dampers, contrarily to traditional dissipative ones, provide a tool to adjust and control the damping coefficient according to the input excitation.

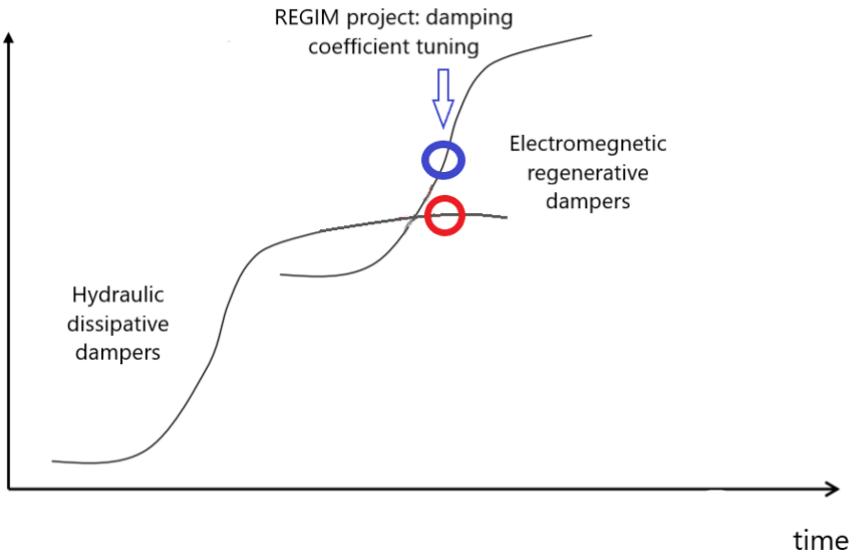

Figure 2.2: S curves of dampers technologies.

Energy recovery is defined as the percentage of otherwise dissipated power which is recovered and stored in the battery. As shown in Fig.2.3, energy recovery represents a novel feature of regenerative dampers, which cannot be compared with the dissipative ones. The research on this technology proceeds in the direction of the optimization of the single components, but further attention should be paid to the overall efficiency, limited by the integration of the sub-components. This is the reason why our current technology is located on the first of a series of possible S-curves, concerning energy recovery performances.

From the technology diffusion point of view in the field of dampers, basing on the variety of applications and the number of startups, the hydraulic damper technology is still the dominant one. REGIM project could improve the technology diffusion by applying an existing technology to a new field of application: agricultural machinery.

The innovation is incremental from the system's viewpoint, as we plan to improve on current technologies and extend their application range to different fields (greater road displacement, higher vibrations) while not changing any of the constitutive components nor their arrangement. In terms of the supra-system the innovation shouldn't bring considerable changes and should be considered modular. We can consider the design to be in the *fluid phase* as many different solutions are being explored, with a promising dominant design in the form of a direct drive electromagnetic generator (tubular permanent magnet linear generator). There is still no market diffusion.

The technology can be considered immature as the research on the individual components is at an advanced stage, but their implementation as a whole system is not yet optimized. The performance of the system still needs to be improved in terms of electrical efficiency and cost efficiency. No radical innovation needs to be performed in the supra-system.

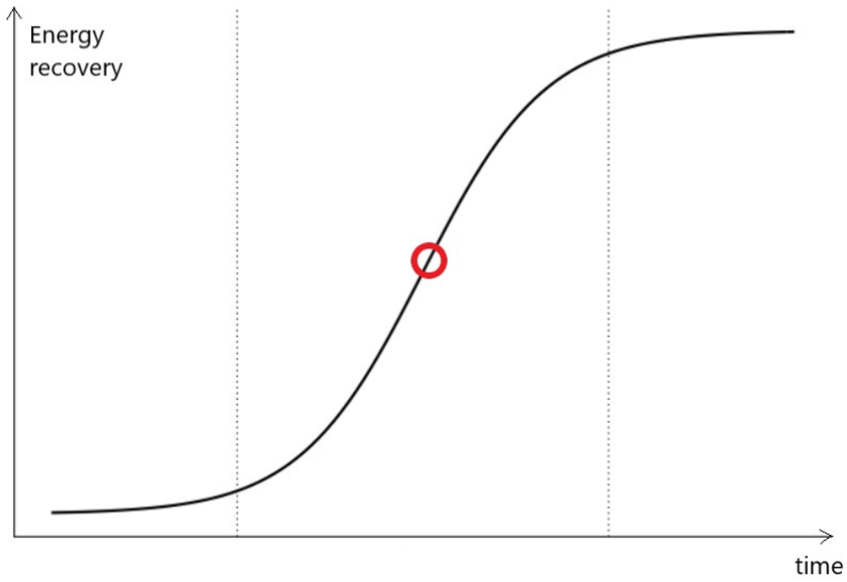

Figure 2.3: S curve of the energy recovery component of regenerative dampers.

Analysing the supply side, the system requires incremental innovation to be performed on itself in order to make it market-ready and effectively shift to the *transition phase*, no radical change is needed in terms of architecture and technical principles. Instead, in terms of sub-systems, components may be borrowed from already existing technologies, but need to be optimized for the application, therefore the most substantial part of the efficiency will be driven by the geometry optimization. In contradiction, the demand side is characterised by a narrow market and the adoption incentives to attract users and investors is based on the sustainable aspect of the product and not on the efficiency savings produced by it. Therefore, the public or private incentives available for the adoption of the technology, like the reduction of taxation when a low carbon footprint is achieved or reduction in taxation for buying components to realize green tech, needs to be exploited.

Inside the paradigm of linear regenerative dampers, two main possibilities have been explored (also described in Chap.3):

1. piezoelectric regenerative dampers;
2. electromagnetic regenerative dampers (direct and indirect-drive, according to the presence of an intermediate linear-to-rotational motion converter).

The piezoelectric design is not considered a suitable solution in the specific field of agricultural environments because it is not able to work with large relative displacements (produced by strongly irregular agricultural soils: thus, it has already been discarded by industry and academia as well. A dominant design for electromagnetic dampers has not emerged yet because the technology is still immature, although each subsystem has already been studied and optimized. This translates to low performance, high cost and production inefficiency. The dominant design that is most likely to emerge is the direct drive for its lower complexity hat will lead to lower cost, lower mechanical losses and higher operating efficiency, both needs of Frandent.

In the field of our project, standards are fundamental as they regulate the inputs and outputs of the system and modular components such as vibration level in the cabin, voltage inputs,

battery capacity. The most relevant existing standard to be taken into account into the design phase of the project is the ISO 16230:2015, which regulates the safety of higher voltage electrical and electronic components for self-propelled agricultural machines. At the same time, the new design interacts with the ISO 8608:2016 concerning the modelling of vibrations from a road surface, and with non-standardized, but common physical characteristics of the components presents specific technical characteristics ranges that are applied to REGIM regenerative damper study.

The project does not aim at changing the existing paradigm of dampers, but in adding additional value to the already existing one. The final product, the damping of the agricultural machine, no longer relies on hydraulic and pneumatic dampers but on regenerative electromagnetic technology, which has already been studied in different fields such as the automotive one. This technology will improve the damping of vibrations and will power some of its subsystems without additional power supplies. Analyzing the the key components responsible for this change, three subsystem are defined: the electromagnetic damper, the electronic power converter and the energy storage system. While all these components are produced by a multitude of companies, the challenge of their integration in an agricultural machine needs to be tackled. By converting otherwise dissipated energy into usable one, this change in the paradigm fulfils the need for minimization of energy waste, making a step towards the realization of a circular economy.

The main competitors for our system are the producers of classical suspension systems, that have productionized dampers that just reduce the vibrations and dynamic loads in the vehicle without converting the kinetic energy into electrical energy. Thusly, the project has a viability for Frandent only if the benefits derived from the use of a regenerative damper would justify the likely higher cost of the components. Among the other possible customers (agricultural machine companies), there may be reluctance in the adoption of REGIM's product for the likely additional costs in changes on the production line, in the cost of the device itself and in the re-design process of their machines.

On the suppliers' side, the elements required to manufacture the product consist of easily available and not extremely expensive components, such as permanent magnets, coils and power converters. It is unlikely that the suppliers would play crucial role for the introduction of our technology, beside the current shortage of electronic components.

REGIM's design requirements have been analyzed based on their importance level to the customer in order to provide optimization and decision boundaries. The requirements are classified on a scale of 1-3 of importance with 1 as the highest value.

Importance	**Requirement**	Feature
1	Current damper dimension	Length of slider ∼60 cm
		Weight 0.8 -1 kg
1	Damping Support of working codition	Damping functioning for agricutural machines that operates within the velocity of 3 to 8 km/h
2	Battery voltage configuration	48V battery recharge
2	Regenerative efficiency	Maximization of harvested energy
3	Cost of production control	Standard sub-components
		Highly available Material

Table 2.2: REGIM's Design Requirements

Chapter 3

Background and State of the Art

A damper is a device that aims at gradually attenuating and stopping the motion along a particular direction. Such action is of interest in all those sectors where strong impulsive motions or vibrations are undesirable or need to be avoided. In the simplest scheme, and considering for simplicity motion along one direction only, such devices consist in a spring to limit the oscillation amplitude and some sort of system capable of generating a stopping force. The operating principle consists in generating a force opposite to the velocity of the motion, that reduces such velocity until it becomes zero. The nature of the force which is exploited may vary, giving rise to different typologies of devices. Most commonly the viscous friction force experienced by a body moving inside a fluid is exploited, and this is at the basis of the most traditional dampers [4, 17], such as those employed in the majority of cars to attenuate the vibrations due to the uneven surface of the road or any impulse that may arise, *e.g.* by hitting a pothole. Another possibility lies in exploiting the *Lorentz Force*, *i.e.* the force experienced by an electrically charged body moving inside a magnetic field. Dampers exploiting such phenomenon are named *Electromagnetic Dampers*. They consist in a moving part, named *Slider*, and a stationary part, named *Stator*. One of the two parts comprises a series of *Permanent Magnets* (PM), separated by ferromagnetic *spacers*, while the other includes one or more phases of copper coils.

Electromagnetic dampers exploit the *electromagnetic induction* phenomenon described by the Faraday-Neumann-Lenz equation

$$\varepsilon = -\frac{\partial \Phi_B}{\partial t}, \tag{3.1}$$

which states that whenever the flux of the magnetic field Φ_B across a surface varies, there will be an induced electromotive force ε, which will tend to generate currents if the medium is a conductor. The idea is that the magnetic field of the PMs will both induce currents inside the coils and interact with them through the Lorentz force. The net effect is a force oriented in the opposite direction to the relative velocity between slider and stator, which then serves the purpose to slow down the motion until such velocity becomes null. From now on, only electromagnetic dampers will be considered, as they allow the recovery of energy in the form of electricity. Within the class of electromagnetic dampers, a few categories might be distinguished: according to how the kinetic energy is dissipated, one can distinguish between *Active*, *Semi-Active* and *Passive* dampers; according to the geometry, *Linear Dampers* and *Rotary Dampers* may be identified; the type of electronic control, according to the exploitation of mechanical sensors, allows to differentiate between *Sensored* and *Sensorless Control*. In the following, a discussion of the different categories will be presented, discussing advantages and disadvantages and outlining the current state of the art. Moreover, considerations on the materials and geometry arrangement in current solutions will be discussed.

3.1 Application fields

In general, all sectors in which considerable vibrations are involved are potential fields of application for energy harvesting with regenerative dampers. Therefore, despite most of the research effort on regenerative electromagnetic dampers have so far been devoted to the automotive field [7, 17–19], the application sectors span a much wider spectrum, including transportation via trucks [20, 21] or trains [20], damping of vibrations in civil structures [22], and power generation from sea waves [23, 24].

In the automotive sector, as well as in transportation, the aim is to recover energy to prolong the autonomy of the vehicle (for electric machines) or to reduce the consumption of fuel. Energy harvesting in tall buildings, instead, exploits both the wind power and vibration power in seismic areas [25]. Indeed, in presence of high winds tall buildings present significant oscillations, which require to be mitigated. Damping systems have been shown to effectively mitigate such unwanted vibrations, in addition to earthquake induced vibrations [26]. Regenerative dampers offer the opportunity to extract energy from such vibrations, that could be used to contribute feeding the buildings' electricity needs. In the power generation sector, instead, the tubular linear generator (on which the energy harvesting in the regenerative damper is based) has been demonstrated and employed as a means to extract wave energy from the sea [23].

In the following, the focus will be put on regenerative dampers mounted on agricultural machines, which is, according to the literature review performed in the first phase of the project, an unexplored field in the application of regenerative dampers.

3.2 Energy harvesting mechanism

The two most common mechanisms for generating electrical energy from vibrational kinetic energy involve piezoelectric materials and electromagnetic generators. Lee et al. [27] designed a shock absorber with two integrated piezoelectric plates, which generate electricity from pressure change induced by a fluidic system inside the cylinder. Their solution produces a small amount of energy and is applicable in small-scale systems only. Xie et al. [28] developed a dual-mass harvester for vehicular suspension systems based on a spring, a moment arm attached with a piezoelectric bar. They discovered that the performance of the energy harvester is largely influenced by the dimensions of the piezoelectric bar, the speed of the vehicle, and the surface roughness of the road. One advantage of piezoelectric converters is that they are compact, portable, and versatile, while still can produce a good power density [28–30].
However, for large-scale applications that involve greater displacements and bigger generators, the electromagnetic approach outperforms the piezoelectric one in the high-frequency range [31]. Therefore, more efforts have been made in research and development of electromagnetic regenerative systems. On top of that, while aiming at recovering as much energy as possible, regenerative shock absorbers still retain their main functionality as a part of the suspension system, that is to improve the performance and ride comfort of passengers. A piezoelectric solution would, therefore, not be suitable for the application in agricultural machines. For this reason, the group focused on developing an **electromagnetic** damper.

3.3 Energy conversion chain

A further categorization of electromagnetic energy harvesters can be defined according to the energy conversion chain [4]. In the *direct drive* solution, magnets and coils are attached directly to the vehicle chassis, and electricity is generated as a result of the relative translational movement

between the magnet core and the coils due to road's irregularities. The *indirect drive* system, on the other hand, relies on amplifying the relative speed of the coils with respect to the PMs, usually converting the translational motion into a rotational one. For optimization of direct drive systems, the efforts are most focused on finding the optimum magnet arrangement with a higher flux gradient per unit mass, as well as the optimum coil profile and the optimum mass distribution of the transducer. Whereas, for the indirect drive system, the focus is placed on increasing the relative speed of the components as much as possible. The indirect drive reduces the driving comfort and handling ability of the vehicle, which makes it an undesirable solution in presence of strong vibrations, as those present for agricultural machines. The investigated solution therefore relies on the **direct drive** approach.

3.4 Control of damping coefficient

According to the way in which the damping coefficient is determined, and the possibility to control it, dampers are categorized as passive, semi-active or active [32].

For a *Passive Damper*, there is no possibility of control of the damping, nor of the amount of harvested energy, since both are set by constraints imposed during the design and fabrication processes.Tthe damping force (*i.e.* the dampers' resistance to extension or contraction) will, therefore, always be the same for a given relative velocity between its components, as defined by the hydraulic or mechanical interactions of its parts.

Semi-Active Dampers, instead, allow to control the damping coefficient of the device in a closed loop. This is achieved by regulating the amount of energy extracted from the vibrations. Thus, semi-Active dampers have a controllable damping force-relative velocity relationship, which allows them to adapt to certain operating conditions.

Active Dampers, instead, are capable of powering, as opposed to merely resisting, a relative velocity in the damper. Thus the efficiency of the damping is greatly increased, improving the driving comfort in vehicles. In this case the energy is no longer recovered from the vibrations, instead it is spent to damp them more efficiently.

The control which is most suited for the requirements of this project, therefore, consists in a **semi-active** damper. In fact, the proposed solution can behave, in principle, like an active damper, but for the purpose of extracting the maximum energy from the vibrations the semi-active behavior is more suitable.

3.5 Geometry

The two main paradigms that can be adopted in terms of electromagnetic damper geometry design are *linear machines* and *rotary machines*. While both solutions are designed to extract kinetic energy from the relative motion of the components, the main difference lies in the direction of such motion. In linear machines, the slider moves linearly (along one direction) with respect to the stator; whereas, in rotary machines, the moving part (named *Rotor*) rotates with respect to the stator. In other words, linear dampers damp linear oscillations, while rotary dampers damp rotations. The array configuration and shape of the permanent magnets and the ferromagnetic spacers depend on the linear or rotational structure.

Tonoli et al. [18,19,33] have provided a theoretical model for the dynamic behaviour of rotary electromagnetic machines and an integral methodology for the design of a possible solution. The dynamic behaviour of such machines can be visualized by studying the mechanical impedance, the ratio between the exerted torque and angular velocity, in the frequency domain. The quantity reads [33]

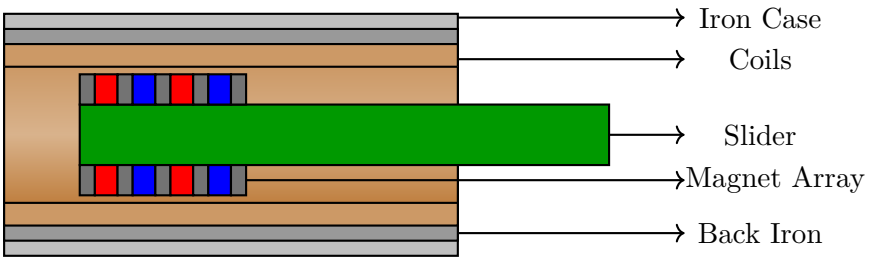

Figure 3.1: Linear Regenerator

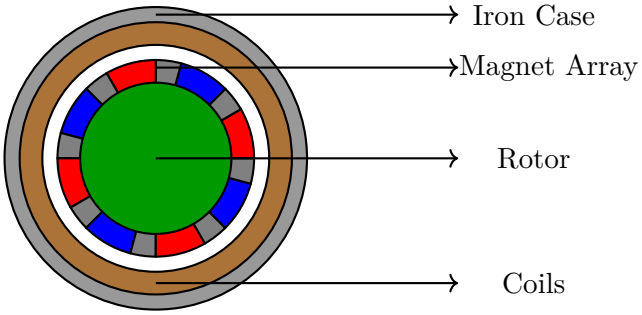

Figure 3.2: Rotary regenerator

$$Z_m(s) = \frac{p\phi_{peak}^2}{R_s(1 + s\frac{L_s}{R_s})}\,, \tag{3.2}$$

where the parameters p, ϕ_{peak}, R_s, L_s are the number of magnetic poles, the maximum magnetic flux density, the coil resistance and the coil inductance, respectively. These parameters represent the design variables which must be tuned to match the design requirements. In particular, the expression of the impedance shows that, after a certain frequency, the machine is no longer able to damp oscillations.

The analysis of *linear* machines is a rather complex task since the number of possible design parameters is large. The lumped magnetic model presented in [34] is able to express the total damping force as a function of the design parameters:

$$F_D = k_f i\,. \tag{3.3}$$

The parameter k_f is the so called force constant and can be expressed in terms of the geometry and magnetic properties of the materials whereas i indicates the current in the coils.

Rotary machines exhibits some advantages. First and foremost, the size of a linear shock absorber is constrained by the maximum amplitude of the oscillations. This means that if larger oscillations must be damped, a larger damper is required, compromising material usage. Moreover, in a linear machine, only the coils that are in front of or close to the magnet array will actively contribute to the damping, thus decreasing the efficiency [18].

However, in the context of automotive applications rotary machines require a mechanical intermediate system to convert linear vibrations into circular oscillations. Often, a gearbox is added to increase the angular speed of the rotational motion. Mechanical converters, however, may induce thermal losses due to undesired frictions, causing loss of efficiency. The **linear**

geometry is therefore adopted for the model, also allowing easier replacement of conventional dampers due to the more similar structure.

3.6 Materials and configuration

To discuss the commonly exploited materials and the configuration of the elements in electromagnetic generators, and in particular in linear electromagnetic generators, it is necessary to refer to the Faraday-Neumann-Lenz equation (Eq.3.1). In order to have an induced electromotive force and therefore to have the ability to harvest the kinetic energy, there needs to be a temporal variation of the magnetic induction flux through the coils (i.e., a variation in time of the "amount" of magnetic field that passes through the coils). The stronger will the magnetic induction field be and the most rapid its variations, the stronger the effect on the induced currents, resulting in a higher harvested power. In a material, the Magnetic Induction Field **B** is linked to the Magnetic Field **H**, by a law named *Constitutive Relation for the Magnetic Field*:

$$\mathbf{B} = \mu_0 \mu_r \mathbf{H}, \tag{3.4}$$

where μ_r is a parameter named *Relative Permeability* of a medium, and indicates how easily the magnetic field tends to flow through that medium. A medium with a high magnetic permeability "attracts" a lot of magnetic induction field, while a medium with low permeability (or high reluctance) will tend to repel them. Therefore, by carefully engineering the various materials used to build the components of the damper, and the arrangement and dimension of such components, it is possible to control how the magnetic induction flux generated by the permanent magnets is channeled inside the device. By maximizing the amount of flux concatenated to the coils (i.e. passing through them), the output recovered power will also be maximized.

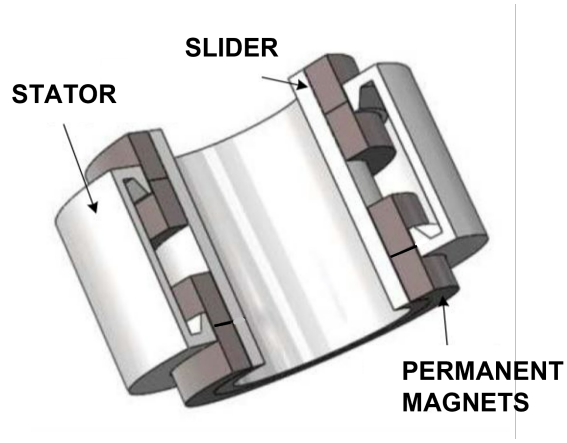

Figure 3.3: Schematic of the structure of a simple model of regenerator [35].

Figure 3.3 shows a simple configuration of the main components of a typical *Tubular Permanent Magnet Linear Generator* (TPMLG). It comprises a slider constituted by a tube on which Permanent Magnets are mounted, and a stator, which includes some structure (that may vary from one prototype to another) which encloses the coils and channels the magnetic induction flux around them. The slider tube has mainly a structural integrity function, and is commonly built in a high reluctance material with good mechanical properties. In [7], PMs are stacked on a 7075 aluminum alloy rod, material which has been extensively used in aircraft structural parts, while in [22] a stainless steel rod was exploited, and was reported to have a greater reluctance and a greater mechanical strength than the aluminum rod. In [10], the material adopted

for the slider tube was a nickle alloy named *Inconel 718*, with great mechanical resistance and high magnetic reluctance. The slider tube acts as a magnetic field concentrator in the region where the coils are present, by repelling the magnetic field from the inner part of the device and focusing it where it can be exploited to generate power.

For what concerns the Permanent Magnets, rare earth PMs are almost exclusively used thanks to their strong generated magnetic flux. Rare earths are a scarce resource and predominantly mined in developing countries, nevertheless alternative and greener solutions are not yet viable as they would result in a drastic decrease of the efficiency of the damper. Usually, Neodimium Iron and Boron ($NdFeB$) alloys are exploited, since they are readily available, cost less in comparison with other rare earth magnets and have a high *remanence magnetization* (i.e., they produce an intense magnetic field).

The back iron and the slots encasing the coils are usually made of ferromagnetic materials, with the intent to maximize the magnetic flux concatenated to the coils. Ferromagnetic materials are characterized by an incredibly high relative permeability (due to the special electronic properties of the materials, in which the electrons act as microscopic magnets all pointing in the same direction) and therefore are perfect for driving the magnetic flux lines around the coils. Nevertheless, the variation of the magnetic induction flux determines an electromotive force in the ferromagnetic components as well, thus generating currents inside them, called *Eddy Currents*. The currents in the ferromagnetic components are not used to harvest power, and instead dissipate energy through the Joule effect (*i.e.* the effect due to which a conductor in which flows a current tends heat up, exploited for instance in incandescence light bulbs). The regenerator aims to recover as much of the kinetic energy as possible, and any losses prove detrimental to its operation. Therefore, it is necessary to use materials with high electrical resistivity (or adopt measures to increase the resistivity of materials, for instance by arranging it in very thin insulated laminations) in order to limit as much as possible the impact of Eddy current losses. In addition to Eddy current losses, there exist two other channels for dissipation of energy in ferromagnetic materials, named *Hysteresis Losses* and *Excess Losses*. Both losses are characteristic of the ferromagnetic behaviour of such materials, described by the magnetic hysteresis loop, which can be modelled through the *Jiles-Atherton model* [36].

The hysteresis losses in particular are due to the energy dissipated for internal resistances of the material to changes in the applied magnetic field. The amount of hysteresis losses is proportional to the area enclosed in the hysteresis loop, since the wider the loop, the more resistance the material will opose to the variations of the magnetic field. Materials with a wide hysteresis loop are named *Hard Ferromagnetic Materials*, while those with a narrow hysteresis loop are named *Soft Ferromagnetic Materials*. The latter respond quite easily to an applied magnetic field and act as to channel it and increase it, they are therefore the category of materials which is used to realise the coil slots and back iron. Hard ferromagnetic materials are instead those with which permanent magnets are realised. In addition to a soft magnetic behavior, characterized by a low *Coercivity* (i.e., low resistance to change of magnetic filed, denoted as H_c shown in figure 3.4), a high *Saturation Magnetization* is required for the operation in electromagnetic generators. The Saturation Magnetization describes how much ferromagnetic material can enhance an external magnetic field, i.e. it gives the maximum magnetic field that the material can generate. Therefore materials with low coercivity (soft magnetic behavior), high saturation magnetization and high electrical resistivity are required for electromagnetic dampers.

In [37], a comprehensive review of soft ferromagnetic materials is proposed. Figure 3.5 highlights the main soft magnetic materials used in power applications and their characteristics.

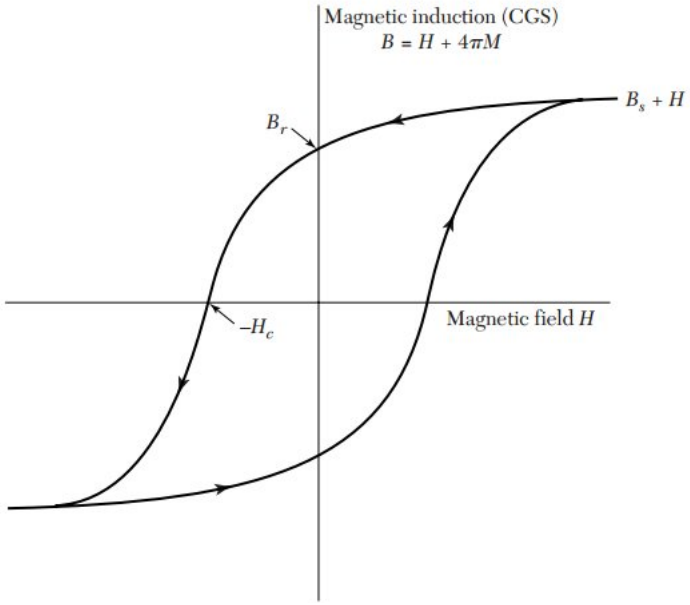

Figure 3.4: Magnetic Hysteresis loop, showing the dependence of the magnetic induction (the quantity appearing in the Faraday-Neumann-Lenz equation 3.1) on the magnetic field. Such dependence is no longer linear as described in equation 3.4, and also depends on previous values of the magnetic field.

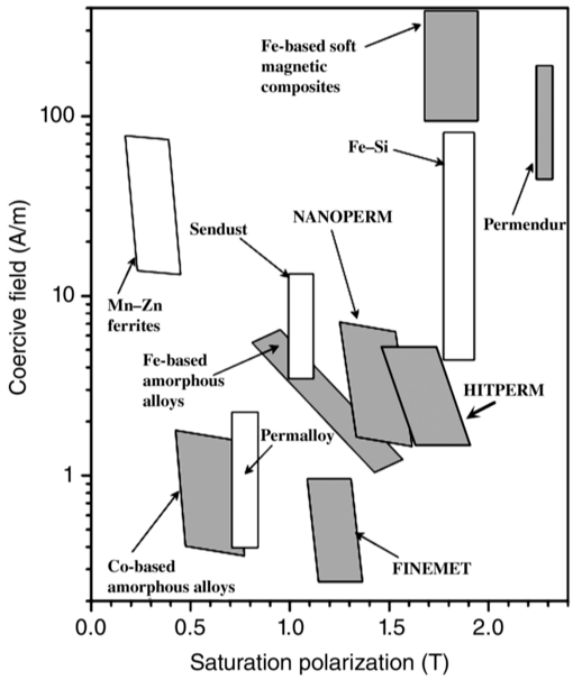

Figure 3.5: Characterization of soft ferromagnetic materials in terms of saturation magnetization and coercive field [38].

Materials that ensure sufficient efficiency of the regenerator are those with saturation polarization at least around $1.5\,\mathrm{T} - 2\,\mathrm{T}$, thus interesting choices include Fe-based soft magnetic compounds [10], Permendur [39], Silicon Steel (Fe-Si) [40, 41], and a wide array of nanocrystalline alloys [42–45].

Iron based soft magnetic materials present high saturation magnetization, but relatively high coercivity and high electrical resistivity, thus resulting in rather high losses. This would not be an issue for non-regenerative dampers or for dampers operating at very low frequencies (e.g., for wave energy conversion, where the main concerns may be resistance of the material to corrosion and highest achievable saturation magnetization), nevertheless for energy harvesting from agricultural vehicles these losses should be minimized.

Permendur has similar attributes, and presents the highest saturation magnetization at 2.35 T. Nevertheless, due to the high losses it is a better fit for those components that need to channel the magnetic flux without experiencing its temporal variations (e.g., spacers between the permanent magnets[1].

Silicon Steel is the material of choice for most devices and is classified according to the concentration of silicon and the crystalline orientation. The Silicon composition ranges rughly from 3% to 6.5%, with the resistivity increasing with the concentration. Nevertheless also the brittleness of the metal grows as the amount of Silicon increases, along with the production costs and complexity. In [41], a thorough review of 6.5% Fe-Si is presented and its favorable properties are compared to those of 3.2% Fe-Si. The former is expected to perform better in terms of losses, nevertheless its availability is lower and its cost is significantly higher.

Nanocrystalline alloys present a wide range of desirable properties in terms of low coercivity and high electrical resistance. During the years their saturation magnetization has also been increased thanks to intense research and is now comparable to that of silicon steel. However, they are still mostly at a research stage and their availability is still limited to laboratory facilities. These materials are a promising solution for future applications, once research has made them available to the market.

According to their availability and cost, the choices for the materials consisted in: **NdFeB** for the PMs; **3.2% Fe-Si** for the back-iron and coil slots; permendur for the spacers between PMs; and **Inconel 718** for the slider tube.

[1] See Chap.3.5

3.7 Power electronic circuit and control

The difference in the electrical characteristics of the generator and load requires electrical circuits as an interface. Fig.3.6 shows a general block diagram of the complete system. The *Energy conversion* block is responsible for adapting the form of electrical energy to better suit the requirements of the load. It must be noticed that, for a bidirectional system like the one designed in this project, power can flow, according to the control, in both directions. In this specific case, it is of interest to operate the system in the *generating mode*, where mechanical energy is subtracted from the damper, converted into electrical energy and again converted into chemical energy inside the battery (battery charging process).

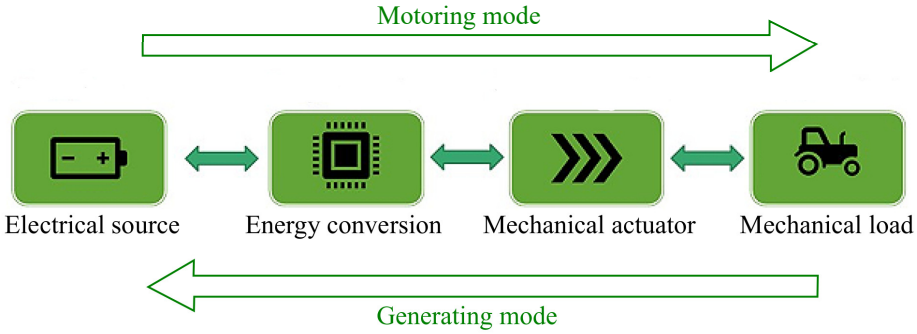

Figure 3.6: Block diagram of a general energy conversion chain.

Due to the nature of the direct-drive system, its output is alternating current (AC). In order to charge a battery, it must be converted into direct current (DC). This can be done by incorporating simple *four-diode rectifier bridges* in the conditioning circuits [7, 46]. The main drawback of this configuration is that the large number of diodes is not suitable for low-voltage applications, and the output waveform should be smoothened out by the use of a capacitive filter. To perform the same AC-DC conversion, Dwari et al. [47] proposed a circuit consisting of one buck converter and one boost converter connected in parallel, achieving higher efficiency compared to rectifier bridges and reducing the voltage drop across the circuit. Dayal et al. [48] designed a topology specifically for low-voltage energy harvesting that reaches up to 55% in efficiency. The topology, utilising a bidirectional MOSFET switch and a split capacitor configuration, operates in *Discontinuous Conduction Mode* in such a way to reduce switching losses, facilitate the control, and reduce harmonic contents. Arroyo et al. [49] developed a new harvesting technique for electromagnetic generators, named *Synchronous Magnetic Flux Extraction* (SFME) method. It switches the electromagnetic element on a storage capacitor at each peak of the magnetic induced current, which will then be discharged to supply the load. Experimental results show that over twice the power can be harvested in the restricted area of the characteristic parameters.

In addition to maximising energy harvesting efficiency, some regenerative shock absorber systems operate in an inverse mode where the external power is used to improve the vehicle dynamics. Hsieh [50] proposed a bi-directional switched-mode rectifier and a control algorithm that can tune the damping coefficient by adjusting the duty cycle of the inverter in the motoring mode, while harvesting the dissipated energy in the regeneration mode. Xie et al. [51] followed a modular approach where a group of generators is connected to the harvesting circuit, and the last generator is used to change the damping coefficient of the system. Roshan et al. [52] employed a three-phase bidirectional converter with a non-linear control method to adjust the input resistance of the converter so that a certain damping coefficient is achieved. The overall

efficiency is computed to be about 77% for the mechanical conversion system, and 78% for the electrical conversion.

Type of electronic control

The Power Electronics group worked towards the design of a converter topology and its relative control to interface the damper with the load. A general block scheme of the machine-battery interface is reported in Fig.3.7.

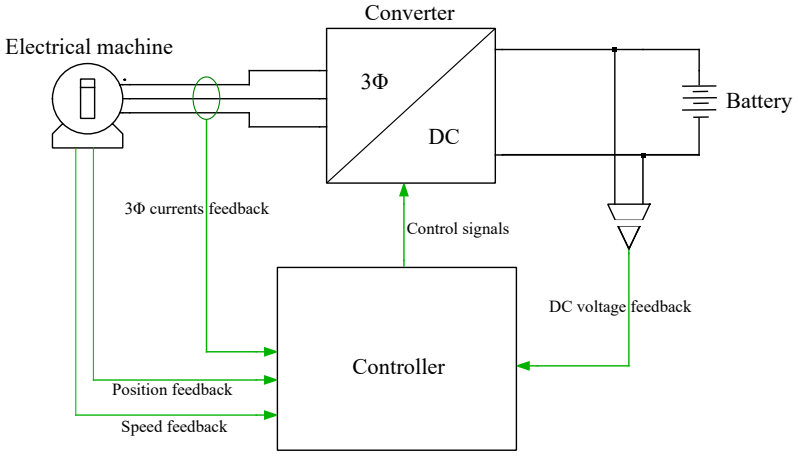

Figure 3.7: Block diagram of the electrical interface between the generator and the battery.

The converter topology choice was, however, limited by the nature of the electrical source: a three-phase (3Φ) electrical motor. The simplest, most versatile and most diffused 3Φ $AC-DC$ converter is the bidirectional 3Φ Voltage-Source Inverter (VSI), shown schematically in Fig.3.8.

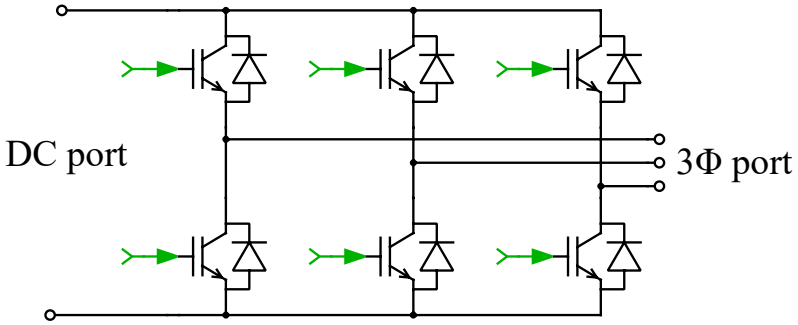

Figure 3.8: Schematic representation of a 3Φ VSI.

This general-purpose converter, coupled with an application-specific control scheme, allows to interface a 3Φ source/load with a DC load/source, providing at the same time the possibility to control the direction of the power flow. In this specific application, since energy harvesting is the goal of the project, the control scheme is designed to provide a net power flow from the electrical machine to the load, providing at the same time mechanical vibrations damping and battery charging.

Thus, the controller design was the main focus of the Power Electronics group. One of the main dichotomy in electrical machines control solution is the exploitation or non-exploitation of sensors for the measurement of instantaneous position and speed. The knowledge, measured or estimated, of these mechanical quantities is in any way necessary to tune at any instant the

generation of control signals by the controller. However, mechanical sensors are typically voluminous, may require to be integrated in the generator structure itself, and are typically expensive.

Control schemes based on the acquisition of instantaneous speed and/or position are called *sensored*. These systems usually exploit electro-mechanical transducers to turn the instantaneous position/speed of the machine into a proportional electrical signal, analog or digital, which is used as a feedback signal for the controller. The measured quantity is compared to an instantaneous speed/position reference, and a properly designed negative feedback loop allows the mechanical quantity to follow the reference one.

The most common solution is the *Field-Oriented Control* (FOC), relying on the measurement of instantaneous position and speed to generate the reference currents adopted in a closed-loop scheme. In [53], the authors use Hall-effect sensors (instead of mechanical absolute encoders) and a PLL to reconstruct the instantaneous angle of a rotational motor. To remove the significant third harmonics in the sensed position, the proposed solution adopts notch filters.

In [54], instead, a *Direct Thrust Force Control* (DTFC) is exploited for a linear PMSM, in which the reference voltages for the power converter are derived by estimating the instantaneous stator flux and rotor force (state variables of the system).

Sensorless controllers, instead, exploit alternative solutions to avoid the need of position/speed sensors. The main principle is to estimate mechanical quantities recurring to a mathematical model of the electrical machine. The accuracy of the control, thus, is strongly dependent on the accuracy of the model: uncertainties on the equivalent electrical circuit model may compromize the robustness of the control [55]. Moreover, the estimation may rely on complex and non-linear computations, requiring high performance Digital-Signal Processors (DSP) of Field-Programmable Gate Arrays (FPGAs). In [56], the authors classify various sensorless controllers according to the open/closed loop scheme and the necessity to measure the initial position, at the startup of the motor.

In [57], the authors exploit an *Extended Kalman filter* (EKF) approach, based on the stochastic derivation of the instantaneous speed and position to run a Permanent-Magnet Synschronous motor (PMSM). The designed control is proved to be robust to physical model parametres variation. Moreover, it can overcome the typical issue of sensorless controls at startup, provided that the model parametres are accurately tuned.

In [58], a *Sliding Mode Observer* (SMO) in which both the speed and the stator resistances are observed variables (estimated) is designed. The novel feature of estimating the stator resistance in the dynamic model makes the system more insensitive to the motor parametres variations.

The adoption, in this work, of a **sensored** control is based on multiple reasons:

- the final application target, agricultural machinery, does not impose strict space constraints which would forbid the presence of mechanical sensors. Of course, as a succeeding step after this project, the structural design should also consider these elements;
- simpler application schemes can more easily be integrated in embedded systems environments, without recurring to DSPs or FPGAs. Due to the lower cost and large availability, microcontrollers-based systems exhibit a larger commercialization potential.

Although, in principle, analog control solutions exist for some power electronics applications, the versatility and ease in re-programming of **digital controllers** make them the most natural solution.

Chapter 4

Solution Design

4.1 Road excitation modelling

Since agricultural vehicles are the target application for REGIM's regenerative damper, it is critical to study the type of excitation that the different ground surfaces can generate and how that excitation is mechanically transmitted to the damper.

Road model

The ISO 8608 standard [59] provides a complete categorization of road qualities in 8 different categories, ranging from A (best *quality*) to H (worst *quality*). The aforementioned standard provides quantitative parameters that can be used to model a particular type of road. It should be remarked that the road profile is a random function and therefore both the amplitude and the frequency of the excitation at each point is unpredictable. What can be predicted is the auto-correlation of that stochastic process, which is usually expressed in frequency domain by means of the *Power Spectral Density* (PSD). The latter is defined as the Fourier Transform of the correlation function and gives a measure of the energy content of each frequency component.

The road classification is performed with respect to the value of its displacement PSD at a particular spacial frequency $n_0 = 0.1$ ([60]).

Road Class	$G_d(n_0)$ **lower bound**	$G_d(n_0)$ **upper bound**
A	-	32
B	32	128
C	128	512
D	512	2048
E	2048	8192
F	8192	32768
G	32768	131072
H	131072	-

Table 4.1: Road quality table.

Table 4.1 contains the numerical value of the coefficients, according to [59], that can be used to reconstruct the road displacement PSD using the following formula.

$$G_d(n) = G_d(n_0)\left(\frac{n}{n_0}\right)^{-2} \tag{4.1}$$

Mechanical model

Once a precise road profile model has been generated, it is crucial to understand how that excitation is transferred to the damper. To compute it, it is necessary to model the suspension

system. Scientific literature contains a plethora of different car models including *full car models* [61] and *stochastic quarter car models* [62]. The simplest model, which is able to produce a first order estimation of the slider displacement and dynamic load applied, is the *quarter car model* employed by Lafarge et al. in [63].

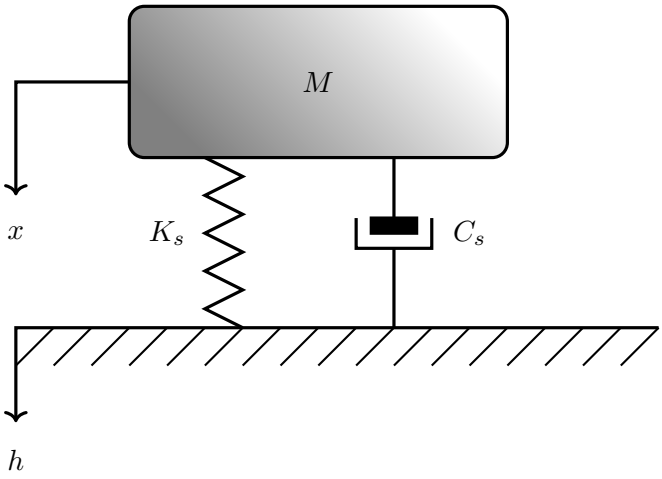

Figure 4.1: Quarter Car Model

The entire car is modelled with a mass M connected to the road via a suspension system. The latter is modelled as a spring-damper system whose properties are the ones of the electromagnetic shock absorber. The equations of motion read

$$M(\ddot{x} + \ddot{h}) + C_s\dot{x} + K_s x = F_D\,. \tag{4.2}$$

In particular; M, C_s, K_s are, respectively, the quarter car suspension mass, residual damping constant and spring constant. These parameters are dictated by the requirements on the dampers performance and are set at the production stage of the damper. The variable h is the road profile displacement (known) while x is the slider displacement (to be determined). The solution of that equation yields the mechanical load and total displacement which have to be sustained by the electromagnetic damper.

On-field data processing

The previous section provided the necessary theoretical framework to understand the mechanical behavior of the damper-system for a generic car. The same system can be adopted to model the response of the regenerative damper in agricultural machines. The stochastic model framed above allows to interpret and extract information from experimental data. In September 2021, an on-field test was carried out in Osasco (TO) to experimentally measure typical displacement excitations applied to a tractor suspension system riding on an agricultural soil. The objective was to derive the spectrum of the displacement in order to define the parametres of the maximum sinusoidal excitation to be tested in simulations and laboratory.
The tests consisted in 4 different rounds of measurements associated to different average speeds of a tractor ($3-4\,$km/h, $5-6\,$km/h, $6-7\,$km/h, $8\,$km/h). To measure the relative displacement, the tests adopted a linear potentiometer (displacement sensor) mounted on the chassis of the tractor. Fig.4.2 and Fig.4.3 show, respectively, the time-domain waveform and the normalized frequency spectrum of the displacement in the 4 testing conditions. What is possible to observe is that, despite not being particularly influential on the maximum displacement amplitude, an increase in the tractor average speed leads to a broadening of the spectrum, *i.e.* higher

frequencies start to appear in the oscillations.
This can be explained by considering the fact that the road profile function remains the same hence an increase in speed will increase the frequency of the excitation seen by the wheel.
In the largest tested speed operation, the main frequency contributions remain confined within few Hz.

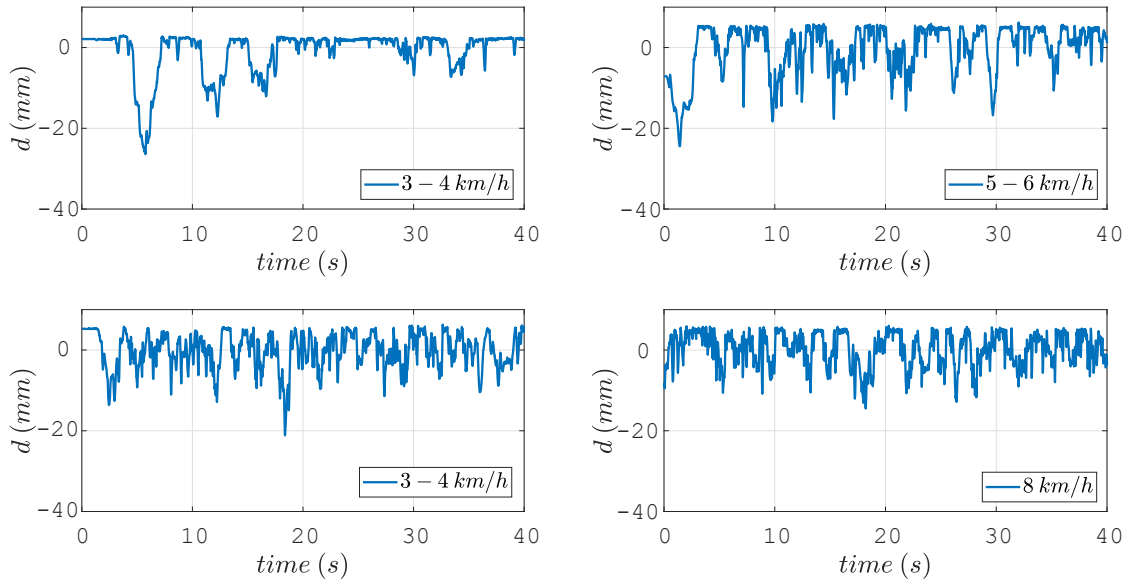

Figure 4.2: Time-domain displacements for 4 different tractor speeds.

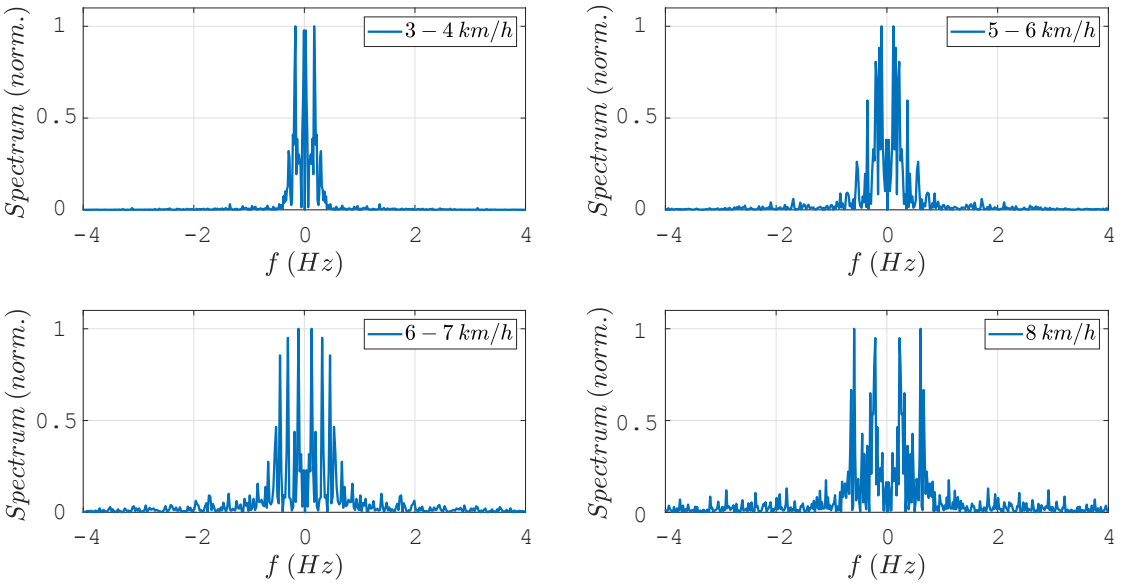

Figure 4.3: Normalized power spectra of the relative displacement for 4 different tractor speeds.

The data provided by the on-field test can be postprocessed in order to obtain the road quality in accordance to the aforementioned ISO standard [59]. The post-processing procedure was performed according to the following strategy

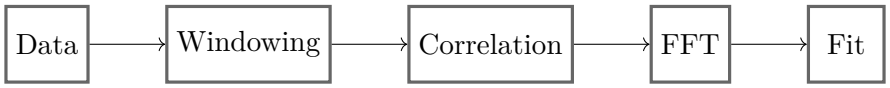

The time series data is converted into a space series data using the tractor velocity. The data is then windowed using a Hanning windowing function (a standard step in digital signal processing which allows to make the signal periodic and achieve peak separation is frequency domain). The correlation integral is then computed and the result is used to compute the FFT, which is the fitted according to the ISO standard [59].

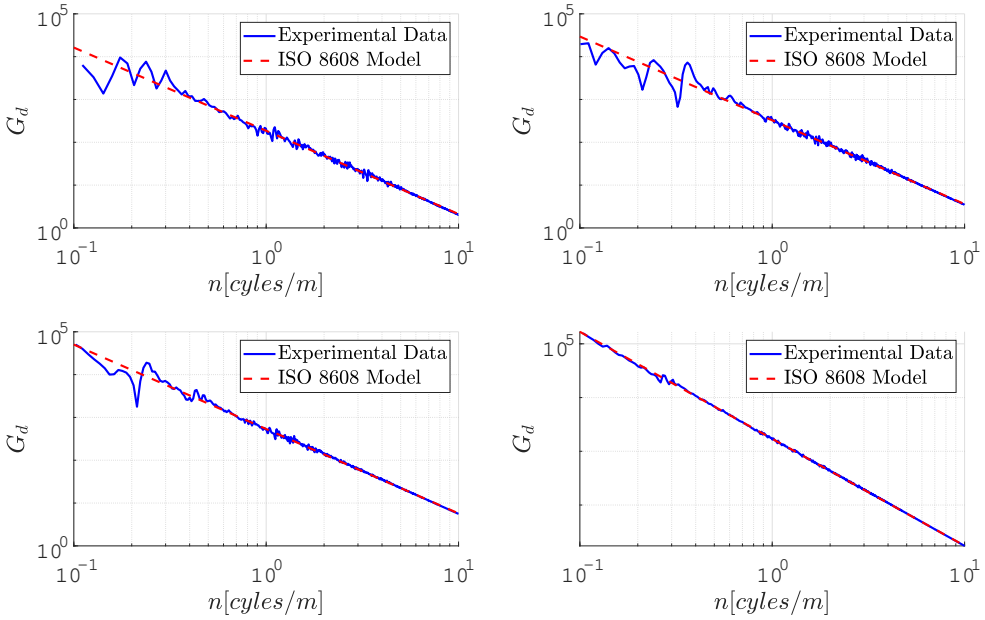

Figure 4.4: Road PSD.

Figure 4.4 shows the result of the aforementioned computation and that the data can be fitted with the ISO model. The measured coefficients $G_d(n_0)$, specified in Table 4.2, show that the tested road is a class C road.

Speed	$\boldsymbol{G_d(n_0)}$
$3-4$ [km/h]	163
$5-6$ [km/h]	295
$6-7$ [km/h]	502
8 [km/h]	315

Table 4.2: Measured coefficients.

The classification of the road quality allowed to extend the validity of the optimization of the damper geometry to other sectors which present similar characteristics. In other words, it defined the range of applications for which the current design is optimized.

4.2 Multiphysics design of the damper

4.2.1 Physical Model

The physics of the linear regenerator is modelled with Maxwell's equations of electrodynamics. The latter provides a set of 8 partial differential equations that fully capture the behaviour of electromagnetic fields in materials. Nevertheless, since the problem is dominated by the effect of magnetic fields, the equations can be simplified into:

$$\begin{cases} \nabla \times \mathbf{H} = \mathbf{J} \\ \nabla \times \mathbf{E} = -\frac{\partial \mathbf{B}}{\partial t} \end{cases} \tag{4.3}$$

The problem is further simplified by the introduction of the magnetic vector potential:

$$\mathbf{B} = -\nabla \times \mathbf{A}\,, \tag{4.4}$$

which allows to express the electric field as:

$$\mathbf{E} = -\frac{\partial \mathbf{A}}{\partial t} \tag{4.5}$$

With this assumption, the system is simplified into a set of 3 scalar partial differential equations which can be expressed in the following vector form:

$$-\nabla^2 \mathbf{A} = \mathbf{J}\,. \tag{4.6}$$

This final equation is discretized by *Comsol Multiphysisc* and solved by means of finite element method on a suitably selected domain, illustrated in Chap.5.

4.2.2 Geometry design

In linear electromagnetic dampers, different possible arrangements of magnets have been studied. According to the direction of the magnetization of the PMs (Figure 4.5), their arrangement can be described as *Axially Magnetized*, *Radially Magnetized*, or a combination of both, named *Hallbach Array* [64]. Iron spacers between magnets can be employed in all configurations, in order to enhance the magnetic flux concatenated to the coils.

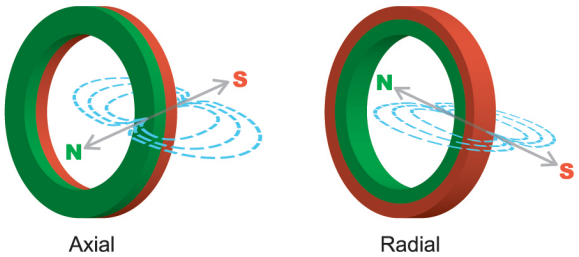

Figure 4.5: Difference between axial and radial magnetization [65].

An **Axial arrangement** of magnets with alternating magnetization, separated by iron poles was chosen for the development of the prototype (Figure 4.6). This choice allows to keep fabrication costs low, while granting the required efficiency of the damper.

The stator, separated from the moving piston by an air gap, is composed by an innermost layer of copper coils enclosed by a back-iron pipe. The purpose of the latter is to concentrate

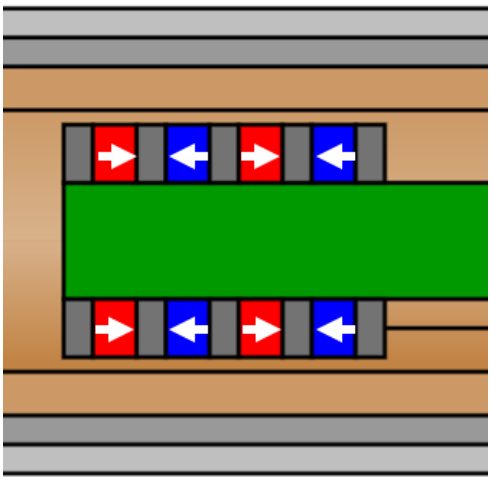

Figure 4.6: Arrangement of Permanent Magnets adopted for the prototype.

the magnetic field over the conductor.

The design activity carried out for this architecture comprehends both the selection of appropriate materials and the optimization of the dimensions of the aforementioned components. The objective is the maximization of the electrical power generated by a movement of the piston. Such an optimization has to respect constraints of size as well as those linked to electronic components' requirements. The size constraints of the architecture are 60 mm for the length of the slider and about $0.8 - 1$ kg for its weight. In order to respect the power electronics' requirements, the wires section have to be chosen accurately. Wires with a higher diameter exhibit lower resistance (which is desirable to increase the extracted power), but fewer coils turns can be allocated for the same available volume, leading to a reduction of the concatenated flux and consequently of the induced voltage. On the other hand, a section that is too small, together with the increased length of the coils resulting from the higher number of turns, would lead to an unacceptable amount of dissipated power because of the high electrical resistance. These discussions are derived from the standard definition of wire resistance:

$$R = \rho \frac{l}{S}\,, \tag{4.7}$$

where ρ, l and S represent the material resistivity, length and section of the wire, respectively.

Furthermore, since the power converter employed can sustain up to 48 V at the coils terminals, a higher generated voltage may be harmful and lead to higher currents than those the power converter and coils themselves can safely operate with. Therefore, the optimization of the coil diameter has to be carried out, keeping in mind the trade-off between efficiency, losses, and requirements of the electronic circuits.

The optimization process was carried out through the following steps. Firstly, *Comsol Multiphysics* simulations indicated that, given the dimensions of the prototype, the configuration for the magnetic core mounted on the slider, which maximizes the recovered power, consists of 4 permanent magnets and 5 iron poles (as shown in Figure 4.7).

The optimization of the damper's dimensions was carried out iteratively and it involved simulations in which the moving piston was subjected to sinusoidal displacements of different amplitudes, coherently with the maximum excitations outlined in the previous section. The simulations were carried out in *passive mode*, *i.e.* the free terminals coils were connected to

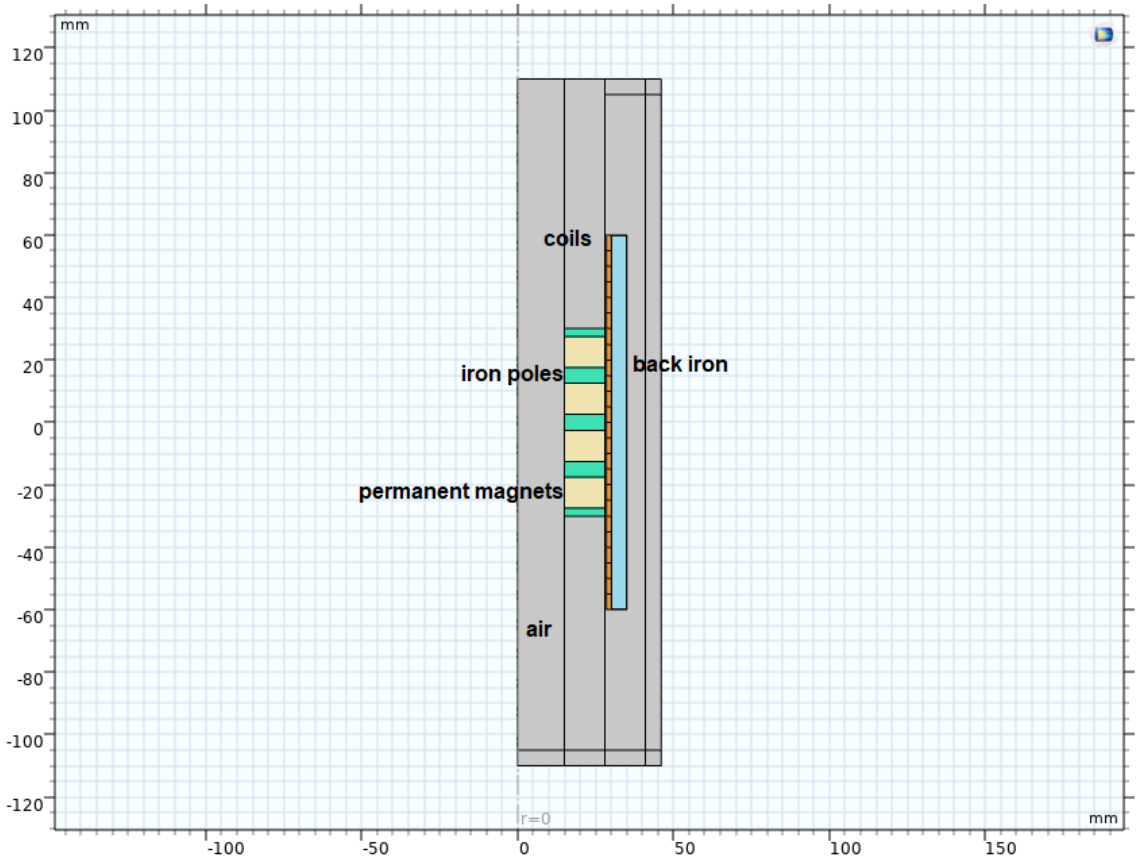

Figure 4.7: Comsol optimized geometry

external resistors equivalent to the coils' resistance. It can be shown that this condition allows to extract the maximum available power, thus constituting the ideal condition that the power converter aims to reproduce. The targets of the optimization consisted in the size of the PMs and iron spacers; the dimensions of the coils slots; the thickness of the back-iron; the diameter of the slider tube.

The obtained generated voltages and powers for each phase were measured and compared. The obtained values are shown in Table 4.3. Figures containing the results of such simulations can be found in Chap.5. Fig.4.7 shows a half-section of the *Comsol Multiphysics* representation of the optimized configuration.

Fig.4.8 and the norm of magnetic flux density generated by a sinusoidal displacement of the slider with an amplitude of 2.5 mm and a frequency of 1 Hz.

Subsequently, the section of the wires was optimized in order to satisfy the aforementioned constraints. In selecting from the standard dimensions provided by the *American Wire Gauge*, a trade-off was necessary, which led to the choice of AWG 26, with a coil diameter of 0.431 mm and resistance of 8.9 Ω. With this coil parameters the 48 V constraint imposed by the battery is respected, as the voltage generated by a sinusoidal displacement with an amplitude of 15 mm and a frequency of 5 Hz (which constitutes the upper boundary for the expected excitation) does not exceed 25 V. This is not the case for the available wires with a smaller cross-section, which would instead lead to higher resistances and violate the voltage constraint of the battery.

Parameter	Value
Mass of the slider [kg]	0.782
Inner diameter of the slider [mm]	30
Outer diameter of the slider [mm]	56
Number of permanent magnets in the array	4
Height of each permanent magnet [mm]	10
Height of the stator [mm]	120
Inner diameter of the coils [mm]	57
Outer diameter of the coils [mm]	60
Height of each multiturn coil [mm]	5
Wires' section diameter [mm]	0.431
Number of turns for each multiturn coil	43
Coil resistance for each phase [Ω]	8.90
Back iron inner diameter [mm]	60
Back iron outer diameter [mm]	70

Table 4.3: Model parameters.

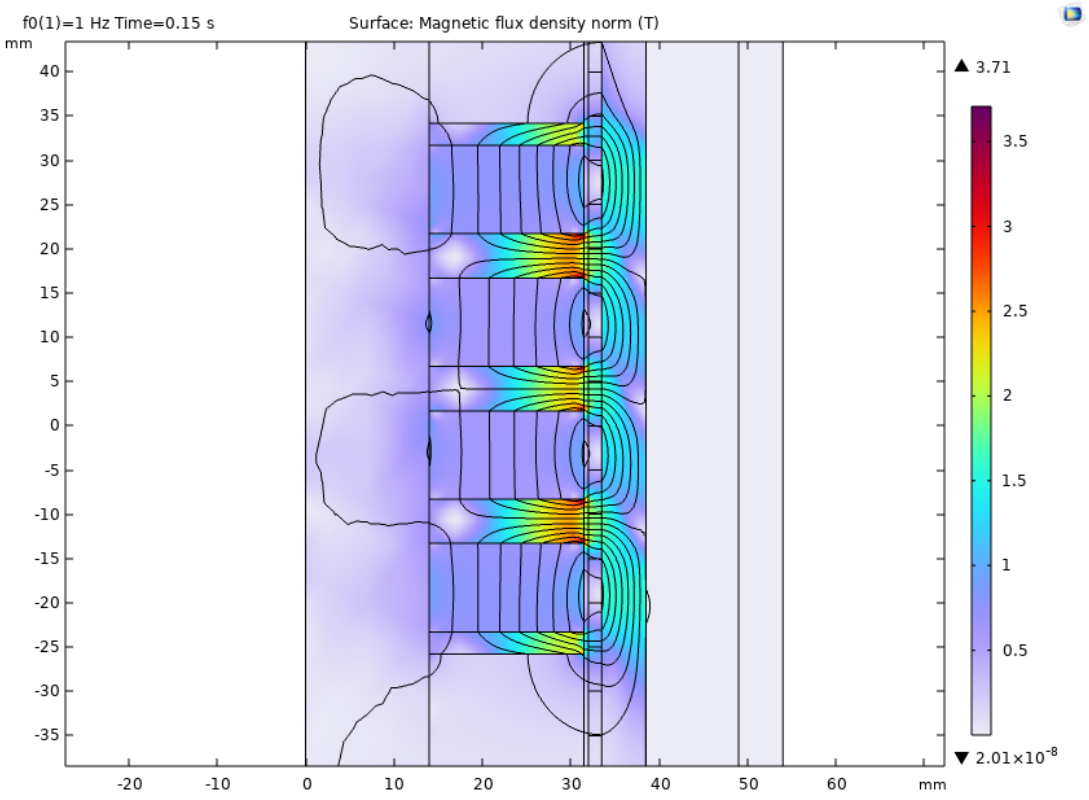

Figure 4.8: Magnetic flux density norm.

4.2.3 Extraction of equivalent circuit model

The output of the design phase is the final geometry of the regenerator. The geometry definition impacts on the electro-mechanical behaviour of the motor, which needs to be described by a mathematical model. This last phase is crucial as it requires a constant exchange of information

between the Multiphysics and Power Electronics groups in order to ensure that both performance and controllability requirements are satisfied.

The inclusion of the regenerator inside a control system requires an accurate knowledge of its dynamics. When dealing with an electromechanical system like this, it is necessary to derive an equivalent circuit model which can well-describe how electrical and mechanical dynamics influence each other. In the case of a 3-phase (3Φ) electrical machine like permanent-magnets rotational or linear motors, a suitable circuit model for each phase is composed of three contributions (Fig.4.9):

- a speed-dependent voltage source which models the back-electromotive force (EMF) induced on the coils from the relative movement of the permanent magnets;
- a series resistance, accounting for the coils ohmic losses;
- a series inductance, modelling the electrical inertia exerted by the generator coils on variations of electrical current.

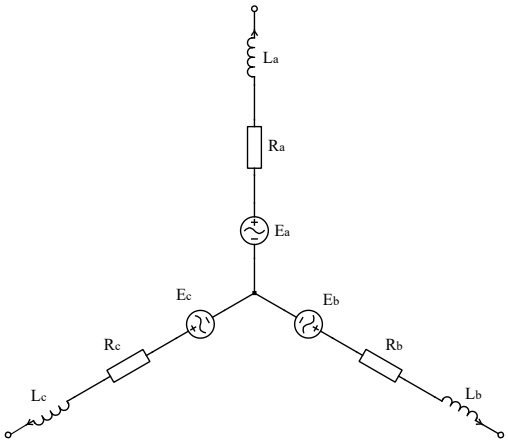

Figure 4.9: Equivalent circuit model of a generic 3Φ electrical machine.

The coils can be *star-connected* or *delta-connected* according to the configuration of the three coils. A star-connection is adopted in this case, and is reported in Fig.4.9.

The closed-loop control for an electrical machine like this can be designed in the three-phase reference frame of the three phases (denoted by *abc*), or in the slider reference frame (denoted by *dq*), which simplifies the design [66]. Since the final goal of the circuit modelling is the ease of the control design process, the description in the *dq* reference frame is preferred. The so-called *Park transform*, relying on the knowledge of the instantaneous position of the slider with respect to the stator, provides a mathematical tool to easily move between the two domains. Thanks to this tool, it is possible to transform the 3Φ circuit model into a set of two equivalent mono-phase circuits in the *d*-axis and *q*-axis [67], as shown in Fig.4.10.

Appendix A reports the set of the 4 fundamental model equations describing the electromechanical dynamics of a linear motor. Among these, the equation describing the dependence of the open-circuit voltages on the slider speed. The other parameters to be extracted for the model are the coil resistance R_s and the d and q line inductances $L_{d,q}$, which have to be computed from the final geometry design choices. In order to achieve this goal, custom simulations

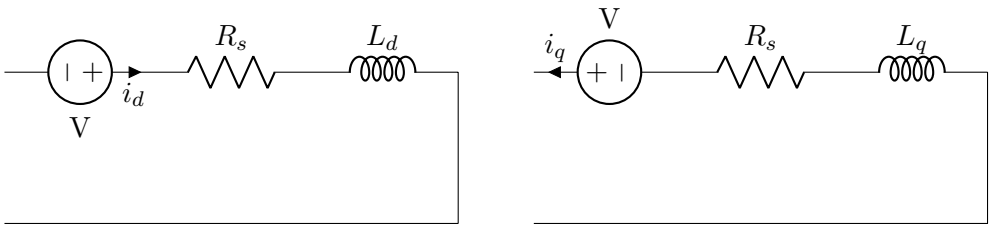

Figure 4.10: The d-q axis equivalent circuits.

have to be designed, performed and post-processed.

Two kinds of simulations are necessary to derive the equivalent circuit model parametres; in both, the slider is kept at a fixed vertical displacement, whereas the coils are connected in a specific configuration according to the test and subjected to a specific external voltage.

DC standstill simulation

Through this simulation, it is possible to extract the resistance of the coils R_s and the time constant of the RL euivalent circuit τ_{RL}. The simulation requires the coils connection represented in Fig.4.11 [68].

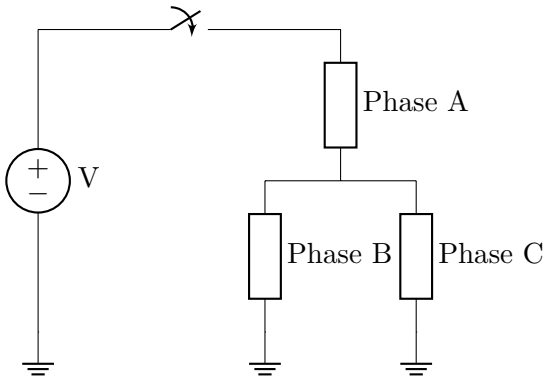

Figure 4.11: The DC standstill test connection.

Coil A must be connected in series with the parallel of coils B and C. Across the free terminals of the phases, a DC voltage source is connected through a switch. When the switch closes, a step voltage is applied. The current and voltage drop across coil A is computed and the waveform data is further post-processed with the use of *MATLAB*.

At steady state, after the initial transient, the current I and voltage V obey the following relationship, that can be used to compute the value of the stator coils resistance, R_s:

$$\frac{3}{2}R_s I = V\,. \tag{4.8}$$

By fitting the waveforms with the exponential function $y(t) = A \cdot exp(-t/\tau_{RL})$ it is possible to compute the time constant of the circuit, from which it is possible to estimate the phase inductance. Repeating the aforementioned procedure for each of the possible displacements of the slider yields the functional dependence of those quantities to the slider position.

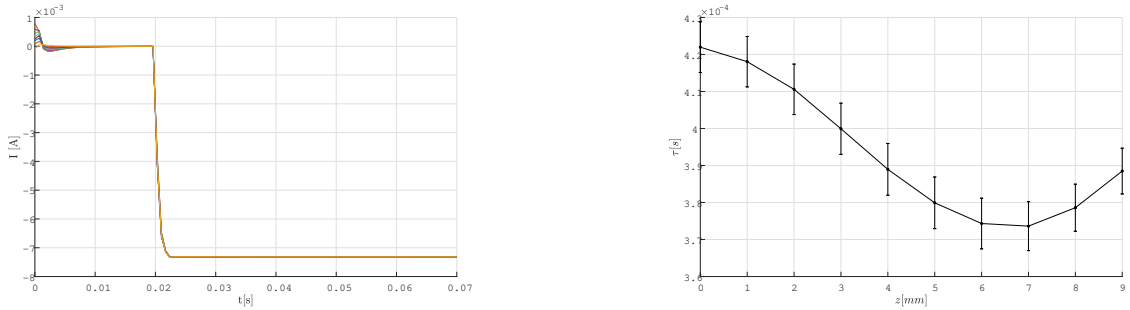

(a) Current Waveform

(b) Time Constant

Figure 4.12: DC Standstill test results

The result show that the functional dependence of the time constant of the circuit with respect to the slider position is well described by a sinusoidal curve. As a consequence, the line inductance is expected to vary sinusoidally as well. The time constant order of magnitude is, from the plot, $\approx 10^2 \mu s$. This value must be taken into account when designing the bandwidth of the control system.

AC standstill test

Another useful test is the AC standstill test [69]. The damper coils have to be connected in similar manner with respect to the DC standstill test.

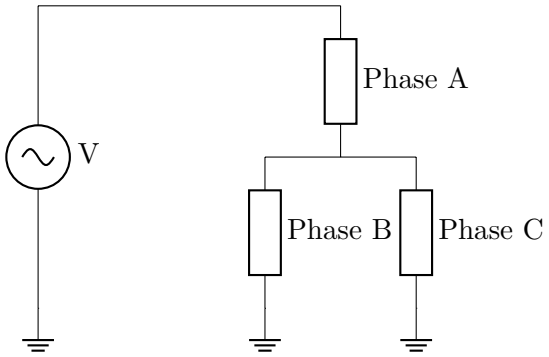

Figure 4.13: The AC standstill test connection

The difference with the previous test is that an AC voltage source with amplitude of 10 V and a frequency of 100 Hz is applied to the coils free terminals. The voltage drop and current across coil A is measured and post-processed.

It can be shown that the total inductance L_L of the system is described by the following equation [69]:

$$L_L = -\frac{2}{3}\frac{V_0 sin(\phi)}{2\pi f I_0}\,, \tag{4.9}$$

in which V_0, I_0 are the voltage and current amplitude respectively and ϕ is their phase difference.

Performing this simulation for different displacements of the slider will yield the line inductance as a function of the coil-magnet relative position. This functional dependence is, by itself, useless as the required parameters are the $d-q$ line inductances. It is possible to show that the aforementioned parameters can be extracted from the line inductance by knowing the functional dependence of the concatenated flux density with respect to the position. Indeed, the d-phase inductance is the line inductance at the position in which the concatenated flux reaches its maximum value and the q-phase at the minimum.

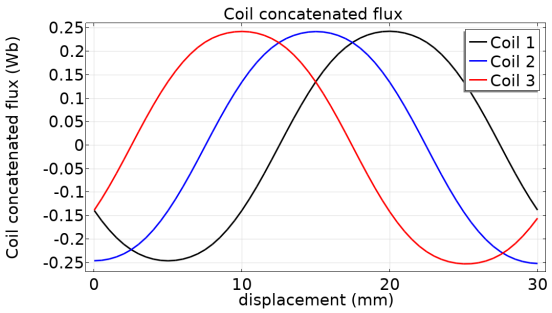

(a) Coil Concatenated Flux as function of the slider position.

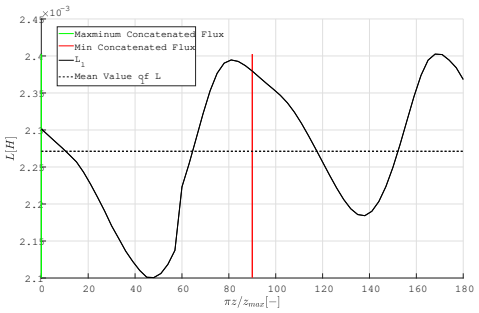

(b) Line Inductance as function of the position

Figure 4.14: AC Standstill test results

4.3 Control design

In this section, the block diagram of the complete control scheme is framed to outline the specific task of each one. The detailed analytical derivation of the key parameters of the control can be found in Appendix A. The general goal of the control scheme is to instantaneously tune the current absorbed by the power converter to realize, as induced effect, an oscillation damping of the regenerator. Every block contributes to this general task with a precise operation.

The mathematical model of the regenerator has already been discussed in the previous section and is further discussed in Appendix A. From the electrical point of view, this control acts to make the power converter behave as an optimal virtual resistance on which closing the regenerator coils. The optimal resistance is the one that maximises the power transfer from the regenerator to the output battery.

As explained, the closed-loop control was designed in the mover reference frame (dq reference frame), allowing a simplification of the design equations. The *Park transform* helps moving easily between the two domains if the instantaneous position is known. Fig.4.15 reports a simplified block diagram including the main building blocks of the designed control system. The control scheme adopted for this work is a sensored Field-Oriented Control (FOC), very common in literature [70, 71]. In general, the control exploits an inner loop for the regulation of the phase currents. The PI controller block (denoted by PI) is fed by the difference between the measured phase currents I_{dq} and the reference currents $I_{ref,dq}$, generated internally in the control board. An external loop generates the reference currents according to the desired damping force to generate.

A brief description of the purpose of the main blocks is presented in the following paragraphs. From the modelling point of view, brushless AC motors, independently from their rotational or

linear geometry, exhibit very similar model equations. As a consequence, the control design in the two cases exhibit strong similarities.

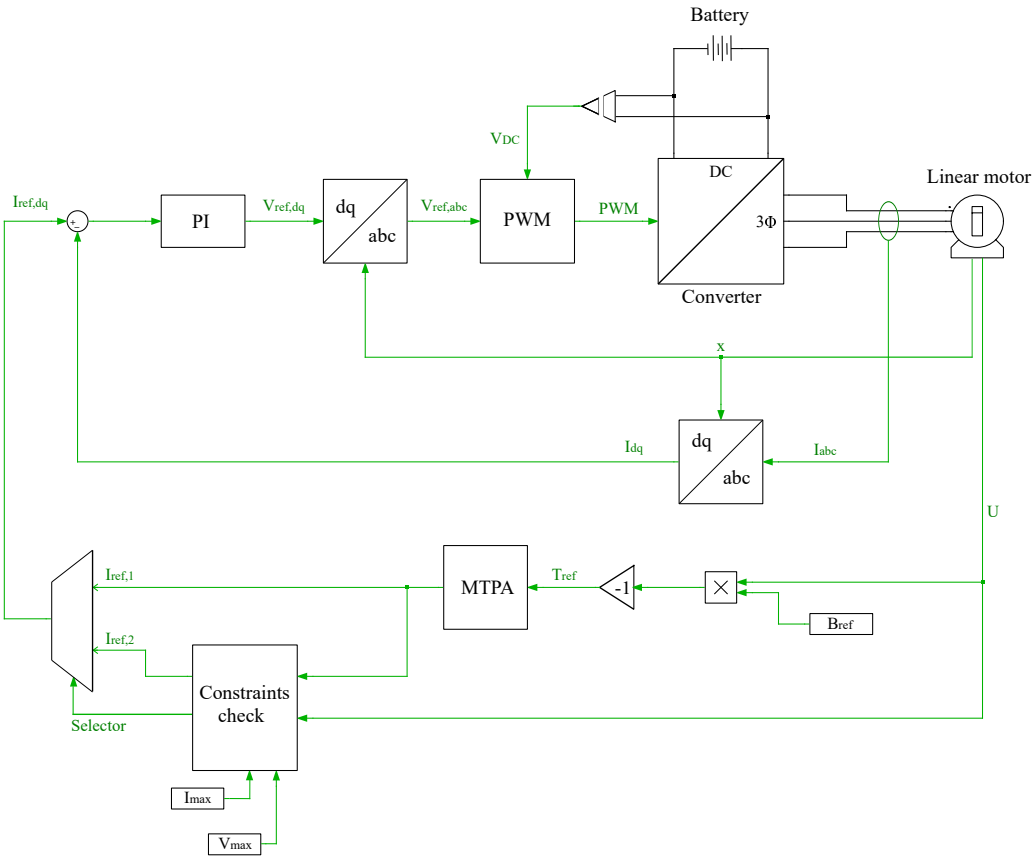

Figure 4.15: Block diagram of the complete control scheme.

Linear motor

In this application, the electrical machine is used as generator, even though, in principle, the control scheme could ensure bidirectional power flow. What is necessary to know of the plant in a control system is its dynamic model, intended as the set of governing equations that describes its electro-mechanical behaviour. The set of four model equations can be found in Appendix A.

MTPA block

The overall goal of the designed *FOC* is to generate an optimal damping force on the regenerator which maximises the damping work (consequently, the extracted power). The damping force can be seen as a viscous friction opposing to the instantaneous movement. The goal of the control is thus to generate, instant by instant, the optimum desired damping thrust:

$$T_{em,ref}(t) = -B_{ref}U(t)\,, \tag{4.10}$$

where the optimum damping coefficient B_{ref} is here assumed to be constant. By convention, the damping coefficient is a positive, real value. The reference damping force, then, requires an additional *minus* sign to take into account the opposing effect. Intuitively, the optimum damping coefficient reflects on the optimum equivalent resistance to achieve the maximum electrical power transfer.

A set of two reference currents $i_{d,ref}$ and $i_{q,ref}$ must be extracted from the reference damping thrust $T_{em,ref}$ according to the electro-mechanical model. The *MTPA* block (*Maximum Thrust Per Ampere*) is designed specifically to generate, among infinite other possibilities, the set of currents maximising the efficiency.

Constraints check block

Before transferring to the PI controllers the reference currents, it is necessary to check if they satisfy the current and voltage limits (I_{max} and V_{max}) imposed by the maximum current capability of the conductors and by the intrinsic voltage limitations of the 3Φ inverter [72], respectively. If not, this block must generate an alternative couple of currents according to another approach, such as field weakening [73]. Appendix A reports a more detailed derivation of the current and voltage limits and a description of the functionality of this block.

PI current controllers

The role of the PI controllers, for this application, is to regulate the phase currents providing a sufficiently high phase margin (for stability purposes) and, at the same time, imposing the desired control bandwidth. While the input of these blocks is the error between measured and reference currents, the outputs are control voltages sent to the pulse-width modulator for the generation of control signals for the inverter. The PI controllers provide at the output the sum of a contribution proportional to the error and one integrating the error in time domain. The goal of the design, presented in Appendix A, is to accurately determine the proportional and integral parameters K_p and K_i according to the desired control bandwidth (500 Hz) and step response.

The results of the design provide the loop gain depicted in Fig.4.16a. The phase margin, approximately 90^o, ensures unconditional stability of the controlled system. Fig.4.16b shows, instead, the closed loop transfer function of the current control: the designed PI parameters set the control bandwidth to approximately 500 Hz, as desired.

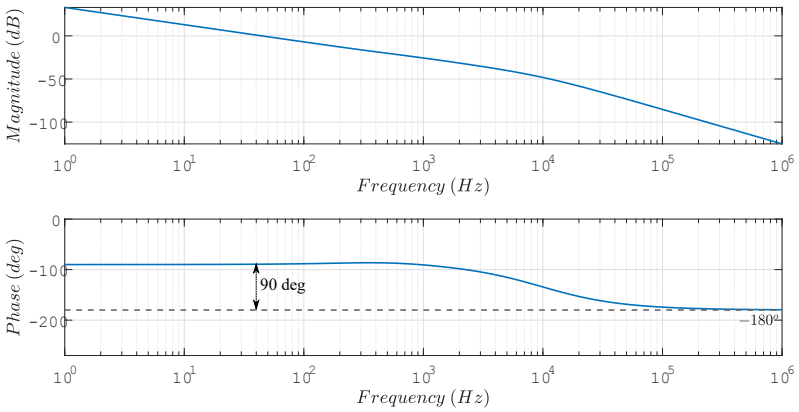

(a) Loop gain of the current control system.

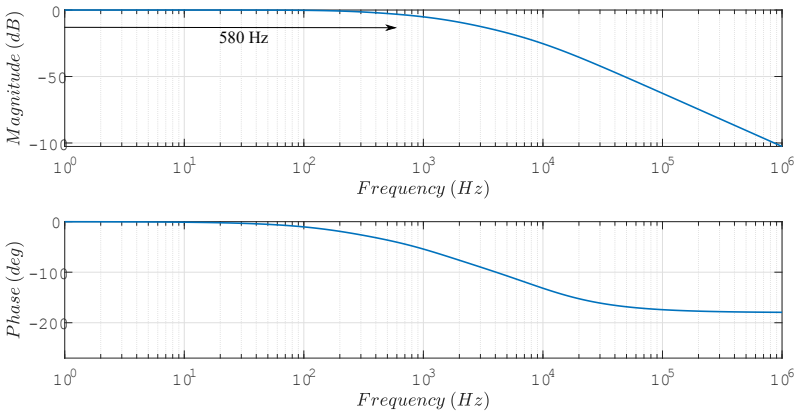

(b) Closed loop transfer function of the current control system.

Figure 4.16: Bode plots results of the design control.

Pulse-Width Modulator

The control voltages generated by the PI controllers, and transformed into their *abc* counterparts, are rescaled by the DC battery voltage and exploited by a carrier-based PWM generator to produce the set of 6 control signals for the inverter (2 for each leg of the inverter). The PWM adopts a 10 kHz carrier, a typical switching frequency for low-power MOSFET-based inverters.

Chapter 5

Results

Once the optimized geometry of the damper had been determined on the basis of the simulations presented in the previous chapter, further simulations were carried out using the software *Comsol Multiphysics* in order to assess the operating performance of the regenerator. *Matlab/Simulink* was, instead, employed to simulate the control system and thus its ability in actively regulating the phase currents to realize the desired damping coefficient and maximize the extracted power.

5.1 *Comsol Multiphysics* simulation results

5.1.1 Computational domain and grid

The equations describing the electromagnetic behaviour of the system (Eq.4.6) are discretised by means of the finite element method into the computational domain. The computation domain is shown in Fig.5.1.

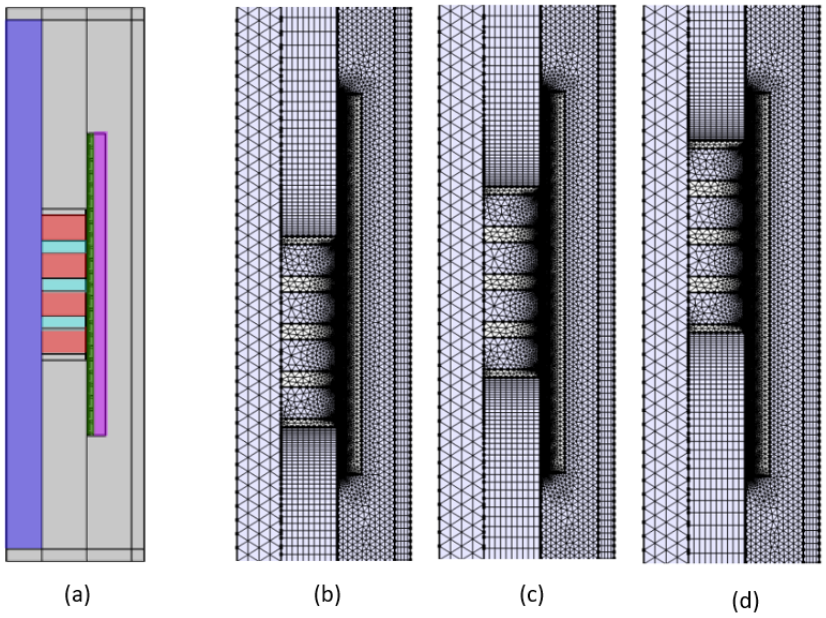

Figure 5.1: Computational domain (a) and computational grid at different slider displacements: negative displacement (b), rest position (c), positive displacement (d).

The moving parts comprise a slider, magnets and iron poles, represented in colour blue, red and light blue, respectively. The stationary parts consist of the coils (green) and back iron (purple). The grey area represents the part of the domain filled with air.

During normal operating conditions, the magnets will slide relative to the coils system. This movement will change the relative position of the parts; the grid is, therefore, required to

dynamically shift and deform during the movement.

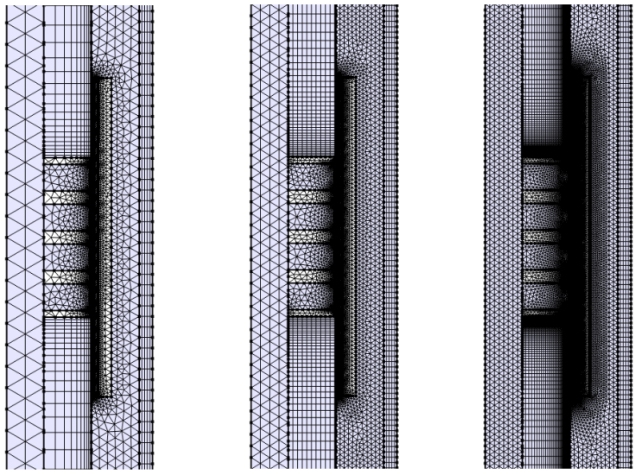

Figure 5.2: Different types of computational grids: (a) Coarse, (b) Normal, (c) Fine.

To achieve a smooth transition and avoid numerical errors due to excessive deformation of the computational elements, the part of the domain over and below the sliding magnets was discretised using a structured quadrilateral mesh, while the rest of the geometry was discretised using unstructured triangular elements. The outer edges of the domain are also discretised with a structured mesh and stretched during the computation. This is done in order to ensure independence from the boundary conditions at the edges of the computational domain (which are arbitrary and should not influence the results). A grid-independence study was performed in order to ensure that the choice of computational grid does not impact on the solutions of the discretised set of physical equations. While, clearly, the finer meshes provide a more accurate result thanks to the better discretisation of the physical space, they also require long computational times. The deviations in the results for the coarse mesh, with respect to the fine one, are, however, within few percentage points (< 10 % even for the more testing simulation conditions). Preliminary studies were therefore obtained using the **coarse mesh**, while those presented in the following correspond to the **normal mesh**.

5.1.2 Simulation results

Comsol Multiphysics simulations were carried out by imposing a sinusoidal displacement of the slider and by measuring the generated voltage, power and damping force. The objective of such simulations was to determine how the characteristics of the displacement, as well as the dimensions of the damper, affect its behaviour. The damper was configured to operate either in **passive mode** (i.e. with external resistances connected to the free terminals) or with an **open circuit** (to determine the generated voltage without any current flow and damping effect).

The first step consisted in evaluating the three-phase behavior of the damper and its **output voltages** under different excitation amplitudes, corresponding to different velocities of the vehicle or to roads with different roughness. The voltage of each phase has thus been simulated under an excitation at a fixed frequency of 2 Hz for different displacement amplitudes.

As the excitation amplitude grows, the output three-phase voltage also increases, starting from a maximum value of 1.2 V for a 2 mm excitation, until above 5 V for displacements of 8 mm. The contribution to the overall voltage from each phase also becomes more uniform upon

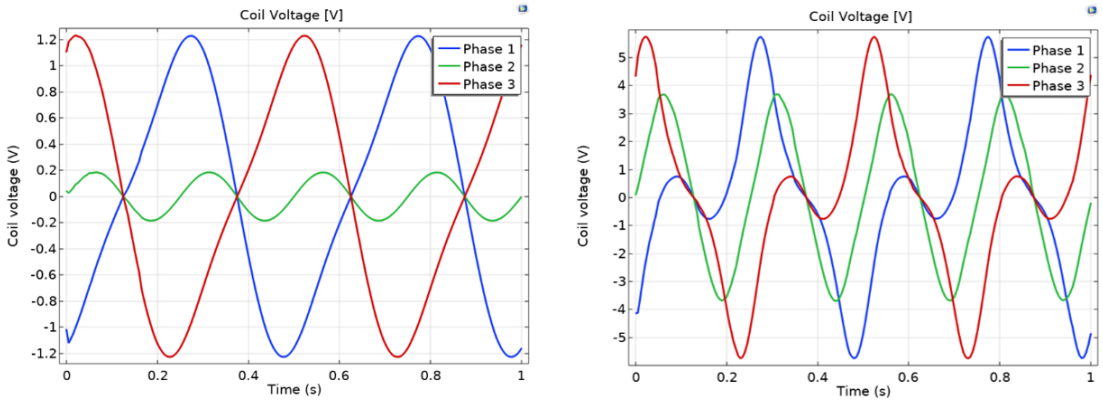

(a) 2 mm displacement amplitude.

(b) 8 mm displacement amplitude.

Figure 5.3: Three-phase voltages generated by a sinusoidal displacement of the slider with fixed frequency (2 Hz) and different amplitudes. The damper is in the open circuit configuration.

increasing the excitation displacements, indicating that the voltage is induced efficiently across all coils.

A second parametric study was carried out to determine the expected **output power** of the physical system under excitation of different amplitude (from 2 mm to 10 mm) and different frequency (from 1 Hz to 5 Hz). The values for the parametric study have been chosen in agreement with the measurements performed by Frandent on the road excitation.

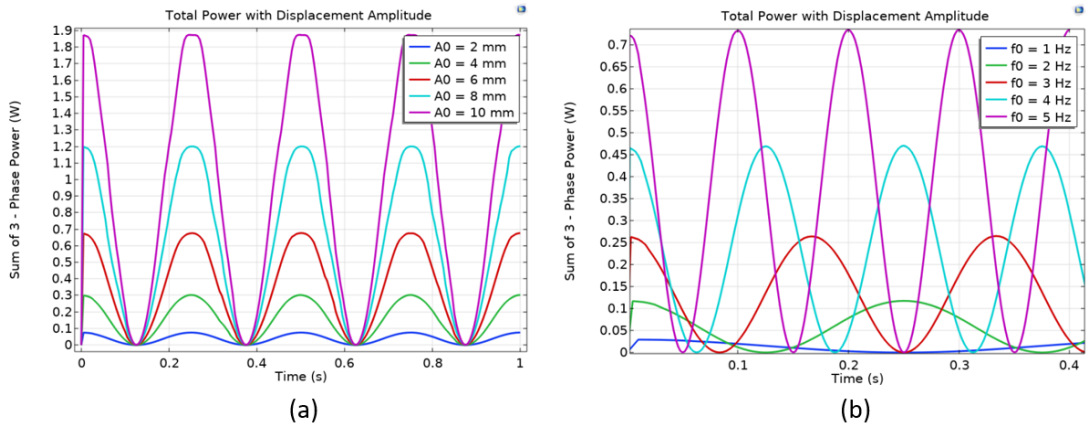

Figure 5.4: Power generated by sinusoidal displacement of the slider with fixed frequency (2 Hz) and variable amplitude (a), and for a fixed displacement amplitude = ± 2.5 mm and variable frequency (b). The damper operates in passive mode.

The simulated power follows the expected trend and increases both with the amplitude and frequency of oscillation, as both determine an increased relative speed of the components with consequent greater harvested power. A peak power of 2 W was obtained for an amplitude of 10 mm at a frequency of 2 Hz. The average value of the physically available power is hard to simulate as the road excitation randomly presents different amplitudes and frequencies at each given position, nevertheless it is reasonable to expect that, under standard conditions, the harvested power is of the order of few watts.

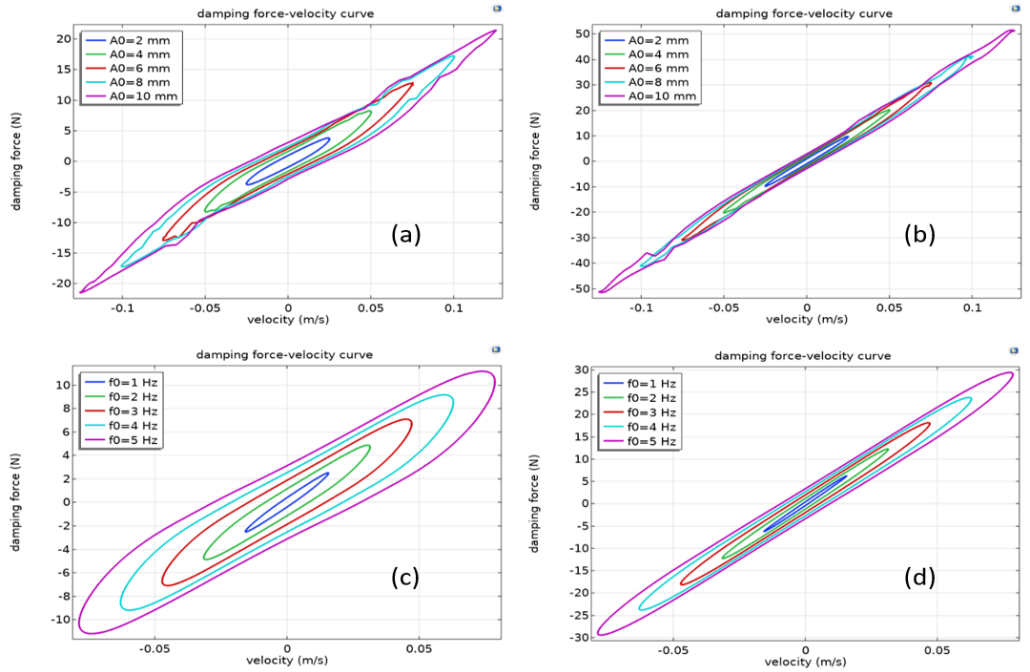

Figure 5.5: Damping force-velocity curves. A comparison is made between the open circuit (left column) and the closed circuit in passive mode (right column) configurations. (a, b): fixed frequency (2 Hz) and variable amplitude. (c,d): fixed amplitude ($\pm$ 2.5 mm) and variable frequency.

To evaluate whether the losses have been properly minimised by appropriate choice of the magnetic materials and of the geometry of the components, the damping force exerted by the back iron was computed and compared to the overall damping force. The curves show an average damping factor of $140 - 160$ Ns/m for the open circuit configuration and of 400 $N \cdot s/m$ for the passive configuration. This difference is due to the fact that in the former configuration the damping is due solely to the currents generated in the back iron, while in the latter there is also the contribution of the coils' currents. The damping in the back iron accounts for roughly 37.5 % of the overall damping of the regenerator. While this value could be reduced by further minimising the losses, it constitutes a reasonable trade-off ensuring to keep the fabrication costs low and maintaining a good harvesting efficiency.

5.1.3 Simulink simulation results

This section reports some of the meaningful results obtained by *Matlab/Simulink* simulations, adopting the control model previously described. All the simulations adopt a fixed-step solver with $\frac{T_{sw}}{20}$ minimum step, where T_{sw} is the switching period. The quantities of interest were moved to the *Matlab* workspace through *To Workspace* blocks to be post-processed. To obtain coherent results with *Comsol* simulations, the displacement excitation is always set to be sinusoidal, with a specified amplitude and frequency.

Fig.5.6 reports the time-domain waveforms of the d-axis and q-axis currents (measured and reference), the three-phase regenerator currents and the averaged charging power. The excitation parameters (oscillation frequency and displacement amplitude) and battery voltage for the simulations are specified in Tab.5.1.

The simulation results are carried out for two operating conditions: on the left column, the

Parameter	Value
f_{osc}	8 Hz
x_{max}	10 mm
V_{batt}	48 V

Table 5.1: Main parametres of the Simulink simulation.

damping coefficient selection ($B_{ref} = 200\,\mathrm{Ns/m}$) meets both voltage and current limits, whereas on the right column ($B_{ref} = 350\,\mathrm{Ns/m}$) the current limit is partially unsatisfied and the q reference current is saturated by the *constraints check* block. Nonetheless, the control well-adapts to this discontinuity and the control provides expected results.

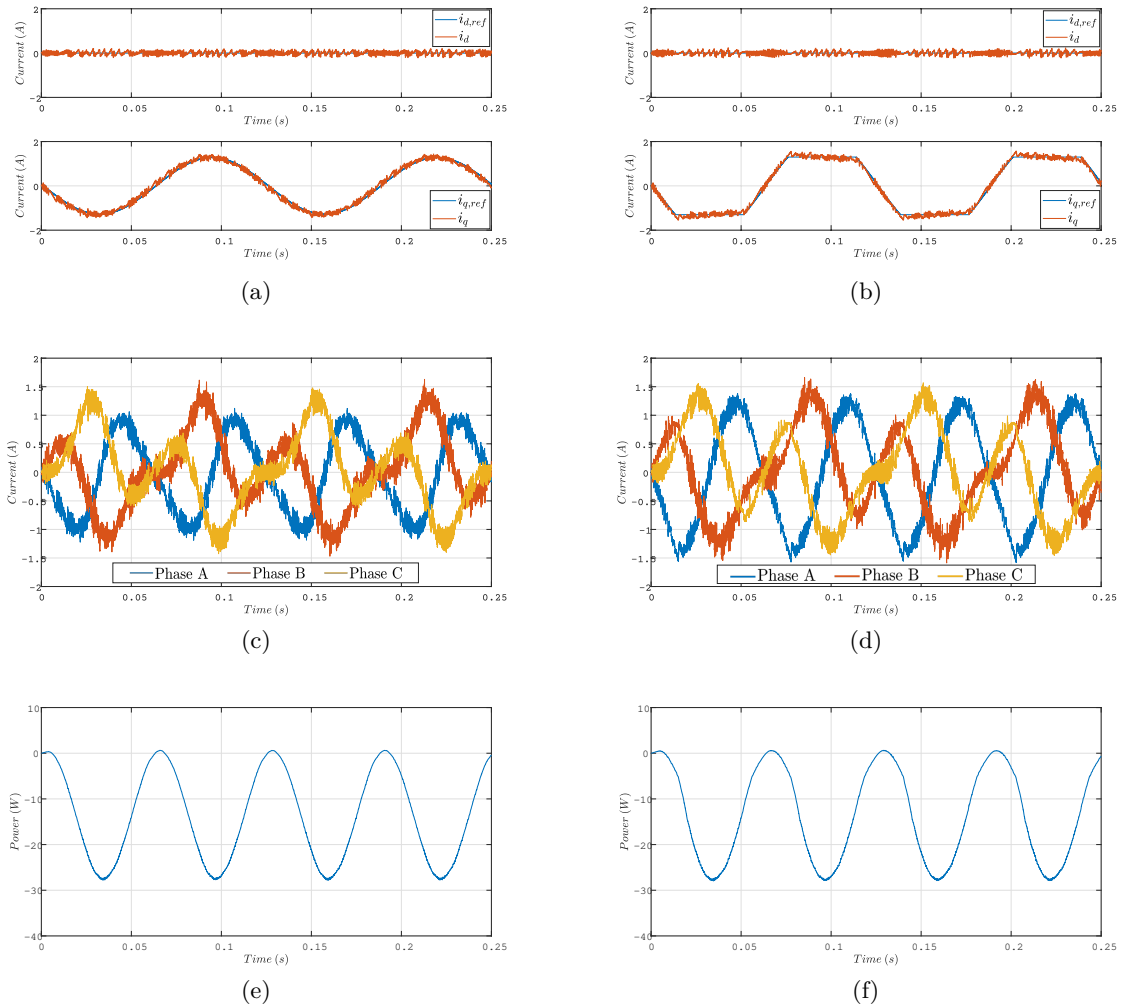

Figure 5.6: Simulated results of the control system in a nominal operation (left column) and saturated current condition (right column): d-axis and q-axis currents (5.6a and 5.6b), phase currents (5.6c and 5.6d), charging power averaged on the switching period (5.6e and 5.6f).

As explained, the damping coefficient B_{ref} defined in the control is linked to the equivalent virtual resistance seen by the regenerator coils. It is possible to prove that the dependence is

hyperbolic [52]:

$$B_{ref} \propto \frac{1}{R_s + R_{eq}} \,. \tag{5.1}$$

The extracted power (charging the battery) represents the amount of power "dissipated" in this equivalent resistances R_{eq}. Tuning iteratively the damping coefficient allows to build the static characteristic $P_{charging}(B_{ref})$ of the system. Figs.5.7a and 5.7b show the behaviour of charging power and dissipated power (in the coils resistances) as functions of the damping coefficient B_{ref} , sweeping from 25 Ns/m to 500 Ns/m. The results refer to a common oscillation amplitude operation (10 mm) and to two different oscillation frequency operations (8 Hz and 4 Hz, respectively).

The following considerations can be drawn:

- For each excitation, there exists a maximum damping coefficient above which the current limit is not met, and the reference q-axis current must be saturated. Above this value, the control cannot provide the exact current needed to realize the desired damping coefficient and the system exits linearity. From the mechanical domain point of view, this means that the oscillations will be damped with a damping force lower than desired;

- Before this boundary, as expected, the power dissipated in the coil resistances follows an increasing, parabolic behaviour (red curves) due to the linearly increasing phase currents:

$$P_{diss} \propto \sum_{k=1,2,3} R_s I_{k,rms}^2 \,. \tag{5.2}$$

  The charging power, instead, exhibits a non-monotonous, parabolic behaviour: the damping coefficient corresponding to the maximum power transfer (the optimal damping coefficient required by this application) is independent from the excitation, but depends on the physical and electrical parameters of the regenerator. For this design, the optimal B_{ref} is around 225 Ns/m. This value could be numerically predicted by analysing the exact open-circuit voltage waveforms of the regenerator, and founding the maximum of the averaged harvested electrical power;

- After the boundary, the shape of the q-axis current approaches more and more a square wave. As such, the *rms* values of the phase currents keep slightly increasing, even though the behaviour of the powers lose their parabolic shape.

5.1.4 Processor-in-the-loop tests

Algorithms and functions to be implemented on an electronic control unit (ECU) are usually developed on a host system using a textual or visual programming *Integrated Development Environment* (IDE). The obtained source files must then be converted into target hardware object files by a dedicated cross compiler, which is a program that translates code written in one programming language into one compatible with a platform different than the one on which the compiler runs. The object files are subsequently linked together to form the file that will be executed on the ECU. To verify the integrity of the compilation process, as well as the numerical equivalence of the code running on the target hardware to the source code, a processor-in-the-loop (PIL) test can be carried out. This test consists in carrying out a simulation in which the physical system is modelled on a dedicated environment, while the controller is run on the target hardware. This test was carried out in this specific case by simulating the gate driver, the inverter and the regenerator using *Simulink*, and by interfacing the latter through serial communication with the evaluation board on which the control algorithm was executed. The

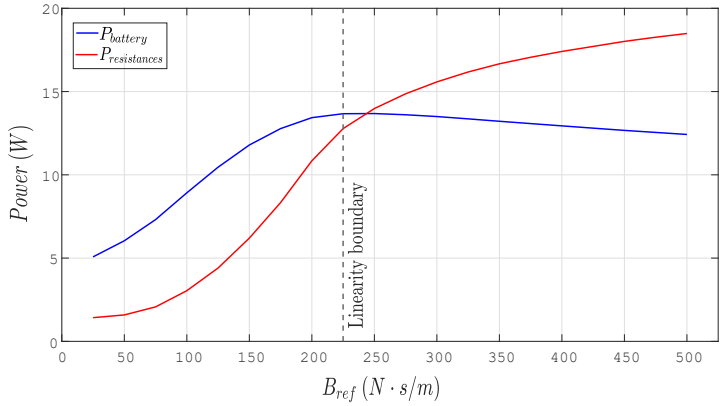

(a) Charging and dissipated powers as function of the damping coefficient ($x_{max} = 1\,\text{cm},\ f_{osc} = 8\,\text{Hz}$).

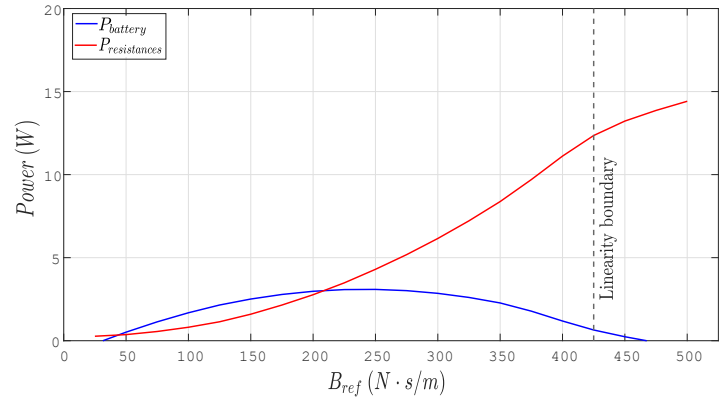

(b) Charging and dissipated powers as function of the damping coefficient ($x_{max} = 1\,\text{cm},\ f_{osc} = 4\,\text{Hz}$).

hardware receives from the *Simulink* model the values of the simulated currents, slider position and battery DC voltage, and after processing them it provides to Simulink the PWM signals to be fed to the gate driver's model. Fig.5.7 shows a block-diagram representation displaying the two mentioned subsystem (the simulated physical model and the hardware) with the relative interface signals.

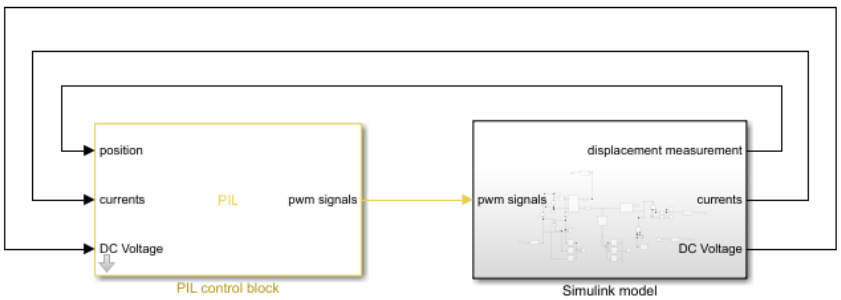

Figure 5.7: Schematic representation of the two blocks of the PIL system.

This phase of the experimental procedure was carried out successfully, and its results were compared to those of an equivalent simulation run on the Simulink model including both the physical model and the control system. The comparison highlighted the close similarity between the two sets of results, observable in the following figures, and thus validated the portability of the control system and its ability to fulfil its main tasks, such as recharging the battery.

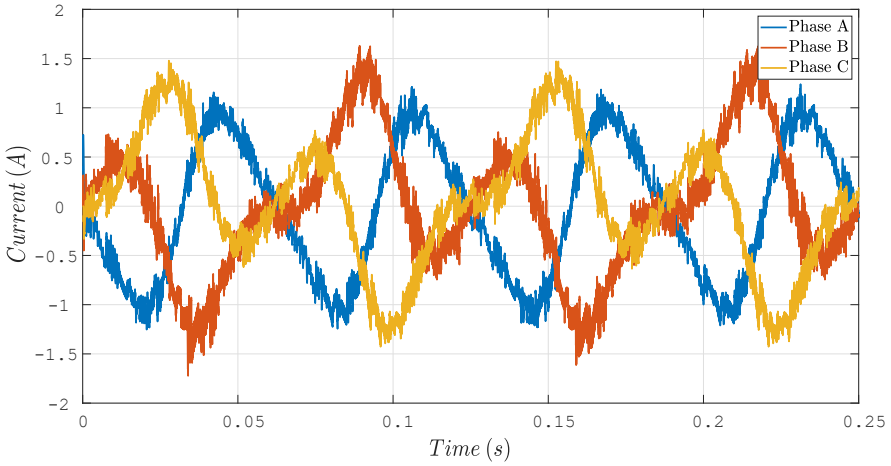

(a) Instantaneous phase currents.

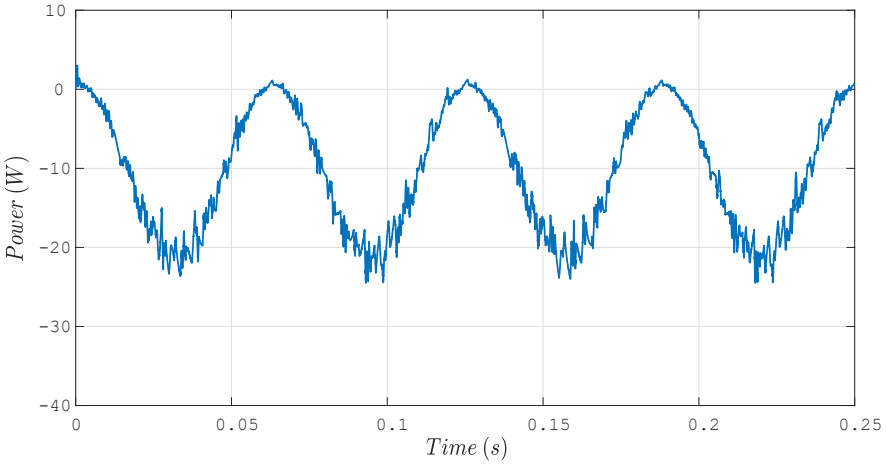

(b) Averaged charging power.

Figure 5.8: Meaningful simulation results obtained with a PIL test referred to a 1 cm, 8 Hz oscillation.

The computer simulations carried out during the design phase identified the optimum geometrical arrangement, size and materials of the components, and electronic control for the application in agricultural machines. The geometrical parameters obtained were provided to an external manufacturing company, along with the selected materials, for the fabrication of the prototype.

5.2 Experimental results

In order to verify the actual feasibility of the design, as well as the aforementioned results, a prototype was manufactured with the goal of testing it on an appropriate test-bench at the Department of Mechanical and Aerospace Engineering (DIMEAS) of Politecnico di Torino. Thanks to the use of proper test instrumentation, the moving piston of the damper can be subjected to mechanical excitations approximating real-world operating conditions. The overall goal of this phase is to physically replicate the operating conditions tested in simulations, an validate the design.

5.2.1 Experimental setup

Control and driver boards

In order to test the functionality of the control scheme, a system of Texas Instrument's LAUNCHXL-F28069M[1] and BOOSTXL-DRV8323RS[2] was assembled. LAUNCHXL-F28069M is an evaluation board from Texas Instrument which is powered by a micro-controller in the C2000 real-time MCU family. It is employed to store all software, communicate with sensors, manage the control of the system, and interface with the damper through the gate driver integrated circuit. The BOOSTXL-DRV8323RS driver board consists of a three-phase half-bridge DC-3ΦAC inverter, which is able to interface electrically the coils of the machine with the battery to be charged. It is directly connected to the evaluation board, and both are powered by the 48 V battery.

This solution has been chosen for its low cost and wide availability, as well as for the presence of MathWorks' "Embedded Coder Support Package for TI 2000". Thanks to the embedded coder, a *Simulink* model could be easily designed, facilitating the handling of data exchange between the evaluation board, the driver, and the sensors. Furthermore, it allows to automatically generate C-code directly from the *Simulink* control model and to download it on the board.

However, this configuration is only suitable for the prototyping phase, as it contains a lot of wiring, and, in absence of proper casing, is not resistance to real working conditions. A specifically designed circuit would be compulsory in order to manufacture a commercial shock absorber.

Sensors

For the measurement of the position of the moving parts, a MLS130 linear displacement sensor[3] is attached to the damper. It is capable of measuring strokes in the $25 - 250\,\text{mm}$ range, and the working principle is the same as a linear potentiometer, where the voltage value is acquired by the analog-to-digital converter (ADC) module on the evaluation board. The displacement value is then numerically differentiated to obtain the instantaneous velocity of the piston (the effect of noise is reduced through adequate low-pass filtering and/or averaging techniques).

It is also necessary to sense the phase currents inside the coils as the inputs to the control algorithm. For this purpose, Hall-effect current sensors are considered since they do not require

[1] https://www.ti.com/tool/LAUNCHXL-F28069M

[2] https://www.ti.com/tool/BOOSTXL-DRV8323RS

[3] https://www.leane.it/sites/default/files/prodotti/MLS130.pdf

internal wiring inside the damper. Digilent's PmodISNS20[4] sensors are suitable for this application, providing a 40 A range, and an accuracy of 2%. The sensor comes with a built-in 12-bit ADC, and interfaces with the controller via the Serial Peripheral Interface (SPI) protocol. The LAUNCHXL-28069M, as a master device, hosts only two SPI modules; therefore, two sensors are used to measure phase currents through two coils, and the third current is calculated from the other two, exploiting the property of the star-connection:

$$\sum_{k=\{A,B,C\}} i_k = 0\,. \tag{5.3}$$

The DVL50[5] voltage transducer is suitable to monitor the supply voltage from the 48 V battery in this application.

Electronic instrumentation

To carry out the characterization of the damper, a digital oscilloscope and a signal generator were used.

The scope is a 4-channel Handyscope HS4, shown in Fig.5.9. It has a maximum sampling frequency of 50 MHz and a 16-bit resolution. The input impedance of the scope is declared to be 1 MΩ.

Figure 5.9: Handyscope HS4

The signal generator is a THURLBY THANDAR TG200 generator (Fig.5.10) that can generate sinusoidal, square and triangular waves up to 1 MHz frequency with maximum 20 V peak to peak. To ensure precise measurements, the output resistances of the generator were measured to be 103 Ω and 692 Ω by means of a simple voltage divider. The 692 Ω termination was used to perform all inductance measurements.

[4] https://digilent.com/reference/_media/reference/pmod/pmodisns20/pmodisns20_rm.pdf

[5] https://www.lem.com/sites/default/files/products_datasheets/dvl_50.pdf

Figure 5.10: Signal Generator

5.3 Experimental procedure

The goal of the experimental phase of this project is to validate the design of the regenerator and control system. This phase is articulated in the following sequential steps.

Characterisation of the regenerator

The design of the control system relies on the mathematical model of the regenerator, specifically the proportional and integral parameters of the PI current controllers, and the *maximum thrust per ampere* block. The more accurate the model is, the easier the tuning procedure of the control design to achieve the desired bandwidth and stability. The characterization goal is to derive the equivalent impedance of the coils (R_s and $L_{d,q}$) and the permanent-magnets flux linkage Φ_{PM}, necessary information to describe the electro-mechanical behaviour of the machine.

Characterisation of the sensors

The role of sensors in this control system is to provide instantaneous feedback about the position of the slider, the phase currents and the battery voltage. Before their actual inclusion in the experimental setup, sensors should be characterized separately to test eventual failures and offsets: the offsets, specifically, can be compensated at a firmware-level. The typical procedure to characterize sensors is to test them in *ad-hoc* situations where the variables of interest (position, current, voltage) can be accurately measured in other ways (for instance, by exploiting a digital multimeter). If the sensor, by datasheet, provides a linear transcharacteristic, few test measurements should be enough to grant a reliable characterization of its response.

Definitive PIL tests

This phase has already been described in the previous section and consists in the upload and testing of the control scheme directly on the microcontroller board, once the characterization of sensors and regenerator has been performed. Although the control board, in these tests,

interfaces with a simulated environment, this phase can be helpful to outline eventual firmware faults before the definitive physical tests.

Mounting and experimental tests

Finally, it is possible to proceed with the experimental tests of the complete system. During the mounting phase, electrical connections with regenerator/battery deserve particular attention to keep the equivalent resistance of the connections as low as possible. Moreover, for signal integrity purposes, it is necessary to minimize the path between sensors outputs and control board pins. Fig.5.11 shows three views of the testbench.

The foreseen tests to be performed can be articulated into 4 successive phases:

1. In the first one, the test-rig generates a sinusoidal mechanical excitation which satisfies the previously mentioned voltage/current constraints (test in a nominal operation). This first test aims at acquiring meaningful waveforms (such as phase currents, line-to-line voltages, charging current) to be compared with the expected results;

2. In the second phase, the test-rig should still generate a sinusoidal excitation. However, the selection of the damping coefficient and of the amplitude and frequency of the excitation is such that the voltage/current constraints are not satisfied (test outside the nominal operation);

3. In a third phase, a sweep test on the excitation frequency would allow to build an experimental $P_{charge}(B_{ref})$ graph to be compared with Figs.5.7a and 5.7b;

4. The prototype is intended to be mounted, for the target application, on the chassis of an agricultural machine and subjected to a complex excitation profile linked to the soil irregularities. As such, a fourth phase should consider a random excitation according to the profiles described in ISO 8608, to reproduce a realistic working condition.

For each of these tests, the objective is to prove the effectiveness of the control system and the efficiency in the energy conversion from mechanical to electrical.

Coils characterisation results

The first phase of the experimental procedure, as described, consists in the characterization of the regenerator, to derive the parameters of its electrical model. Actually, due to temporary unavailability of materials, the prototype was manufactured with a different conductor section with respect to the one designed and exploited in all *Comsol* simulations (AWG 30 instead of AWG 26). Moreover, a manufacturing defect caused the coil of one phase to be broken and, as such, not suited to be tested in the expected scenario. The thinner wire, beside reducing the current capacity (and then, limiting the maximum operating excitation), is expected to provide different results in terms of coil resistance and inductance. As a consequence, the experimental results reported in this section do not claim to validate the simulation results, but to present and validate the experimental procedure for the extraction and processing of data.

The value of the inductance of the coils is of paramount importance for control purposes, allowing to tune the PI controllers parameters; therefore, ensuring the value is close to the one chosen during the design phase is a requirement. Since the coil behaves as series of a resistor and an inductor, the impedance, in the Laplace domain, is $R + sL$. Feeding an input sinusoidal voltage with swept frequency and measuring the output voltage with a scope will allow the investigation of the circuit's transfer function. The measurement setup is shown in Fig.5.12.

(a) Regenerator prototype and displacement sensor mounted on the test-rig.

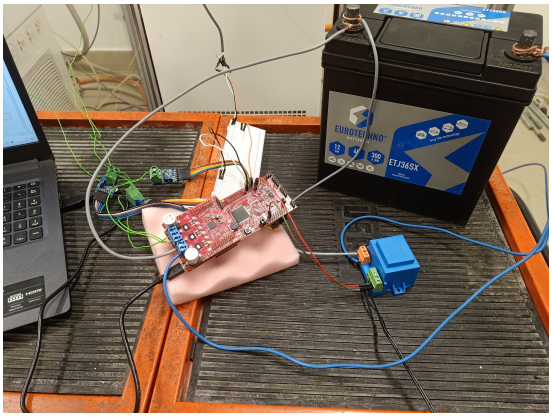

(b) Evaluation board, a 12 V battery, current and voltage sensors.

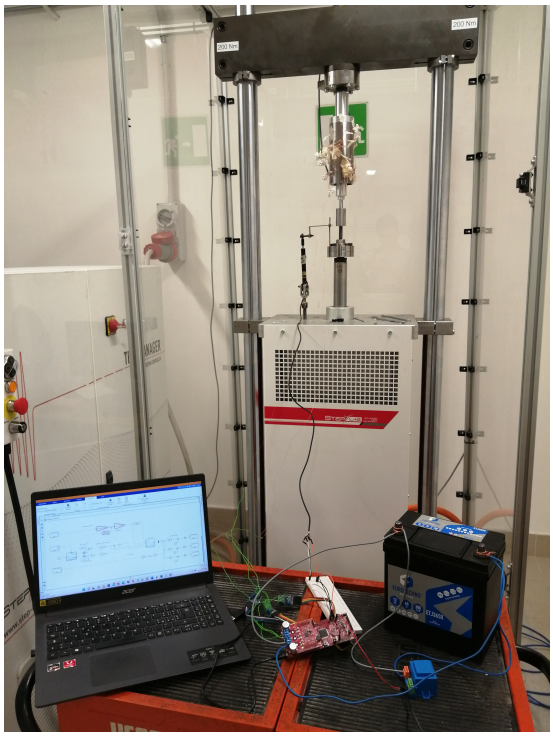

(c) Complete testbench.

Figure 5.11: Views of the testbench.

Assuming a very large input impedance of the scope, the output voltage is related to the input voltage by

$$V_{out}(s) = \frac{R_s + sL_s}{R_s + R_{out} + sL_s} V_{in}(s)\,. \tag{5.4}$$

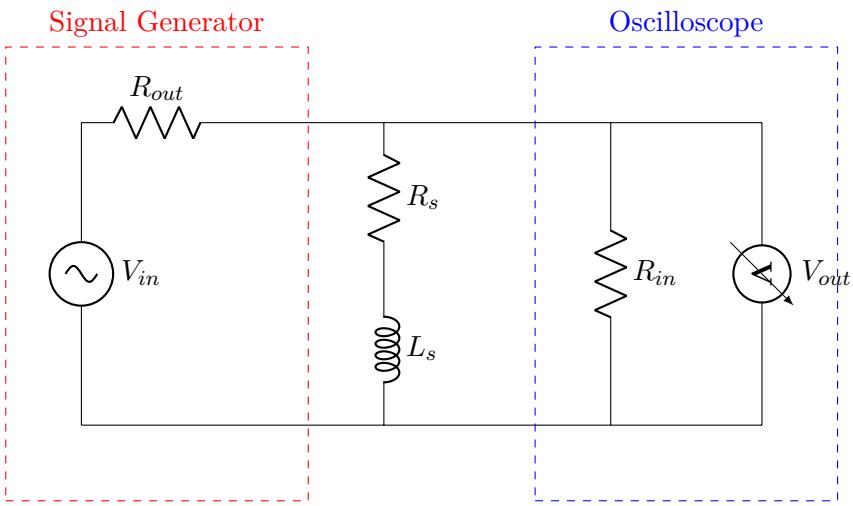

Figure 5.12: Measurement setup for the coils characerization.

The inversion of Eq.5.4 will yield the value of the coil impedance $R_s + sL_s$ at different frequencies. The fitting of the measured values through Eq.5.4 brought to the impedance graph in Fig.5.13.

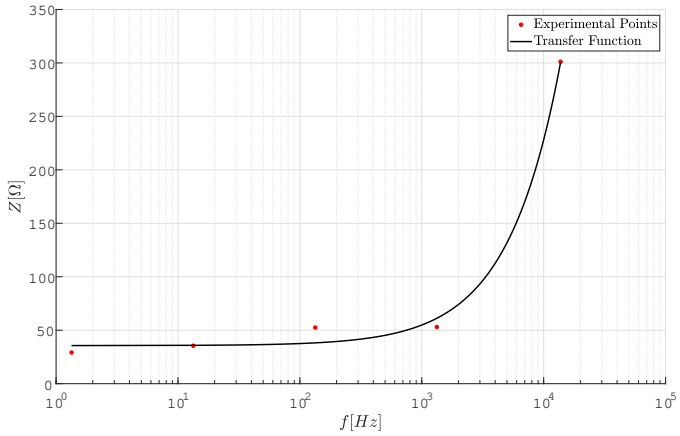

Figure 5.13: Experimental and fit coil impedance.

Clearly, the obtained results (reported in Tab.5.2) for the coil resistance and inductance, do not match the results of *Comsol Multiphysics* simulations, due to the different conductor section and number of coil turns for each phase.

Parameter	**Value**
R_s	$30\,\Omega$
L_s	$4.3\,\text{mH}$

Table 5.2: Coil Characterization results.

Chapter 6

Conclusions

The goal of this project was to prove the feasibility and measure the performances of an energy harvester prototype for agricultural applications. The product is designed to damp the oscillations of an agricultural machine, and convert the subtracted energy to recharge a 48 V battery. The replacement of traditional, passive suspensions with this active system would allow to harvest energy otherwise dissipated in heat. The battery charging feature, moreover, provides an attractive solution in perspective of a massive electrification of agricultural field.

This work considers both the physical design of the machine and its electronic control. The physical design followed an iterative approach to determine the regenerator dimensions according to the maximisation of power generation, without neglecting size constraints imposed by the target application. COMSOL Multiphysics simulations were carried out to tune the geometry. The other achievement of this work was the design of an ad-hoc electronic control system to maximise the power transfer from the regenerator to a battery. The simulations were intended to be validated by an experimental testing session, but a prototype defect made it impossible to proceed with it.

Actually, due to time constraints, the research may proceed in the possible future developments after the conclusion of this project:

- **PCB-based electronic control**. As explained, the electronic setup was based on an evaluation board by *Texas Instruments* interfaced with discrete, panel-mounted sensors. This simple solution allowed to accelerate the design process, but does not ensure the maximum reliability nor the best compactness. In the last decades, printed circuit board (PCB) solutions have become more and more interesting in the market thanks to the possibility to realize high power density circuits. The minimization of connection traces allows to reduce resistive parasitics. Moreover, since all the sensors (except for the displacement sensor) would be soldered together on the same board, the reliability of the complete system would increase: the board would be more resistant to the excitations of a moving tractor or other agricultural machine. The PCB implementation of the control system could be one of the possible improvements of the project;

- **tests on realistic mechanical excitations**. The lab testing session was conceived to test the effectiveness of the control under purely sinusoidal excitations. An intermediate step before the integration of the system to a real machine chassis would be to test the effectiveness of the control and the power harvesting potential with a more realistic, random mechanical excitation;

- **improved control for driver comfort**. In this work, the objective of the control is to maximise the power transfer, by properly selecting, in advance, the equivalent damping coefficient to realize. An improved version of the control algorithm could take into account the driver's comfort, by analysing, for instance, the impact of the oscillation damping on the driver's seat.

The impact of the project can be evaluated on the CO_2 footprint decrease and the cost decrease within a long term ROI. The real condition test within Frandent "Shock track" will be able to quantify and validate the energy harvesting power. Nevertheless, the lock-in of technology will be overcome when the installation of the designed device within the agricultural machine will be completed. The design will be expanded with a study on the Geometry Dimensioning and Tolerancing (GD&T) with the production team in order to finalize the components needed and the procurement. In addition to GD&T study, an evaluation of the impact to existing components will need to be revised to include the new damper. While no other major changes will be required, transformation for the battery cabling is needed. These steps are enablers to the productionization inclusion, the ability to power part of active elements of the agricultural machine will evaluate the results on the final product. Research on auxiliary equipment of agricultural machines was carried out and the impact of the electrification of those part amounted at 278 million liters of fuel saved early only in the us market [74], therefore the productionization of REGIM device could contribute to an actual reduction of CO_2 emission within the agricultural sector, that currently drives around 21% of the world carbon dioxide emission [75].

We can conclude that the project was able to deliver a clear result that will enable the creation of a value chain within Frandent and its stakeholders environment. While the journey towards the full electrification of agricultural machines is still long, the contribution the project leaves is the technological introduction of a new wave of dampers for the agricultural industry. Its active impact on the society is connected to its expansion and support from the parties involved.

The REGIM team hopes that this technological progress will lead the way for further research and expansion, towards sustainable mechanization. We are committed in publishing the finding to let other take the step even further. We hope to see regenerative dampers adoption become the norm in the field and in others as well and we feel honored to have contributed in part of this change.

Appendix A

Analytic control design

This appendix reports more technical details about the design procedure for the definition of the PI parameters of the control system. The following procedure is referenced to the block diagram shown in Fig.4.15.

A.1 Model of the plant

First of all, it is necessary to detail the electro-mechanical model of the plant. The analytical model of a linear brushless AC motor can be found in several references, like in [70]. For simplification purposes, it is common to describe three-phase systems like this mover reference frame. In this domain, time-varying 3Φ electrical quantities can be described in terms of the projections of a time-varying $2D$ vector (the *space vector*) on time-varying axes that are synchronized with the mover motion ([66]). The so-called *Park transform*, performed by $abc - dq$ blocks, offers a straightforward mathematical tool to move from the traditional abc reference frame to the dq vector representation. Thanks to the reduced number of controlled variables, the entire control scheme is simplified if designed in the dq reference frame. Moreover, at steady-state condition, 3Φ sinusoidal quantities are represented in the dq domain by two DC quantities, further simplifying their management [76].

Four equations (Eq.A.1) are necessary to define the complete mathematical model of a linear machine ([77–79]):

- the electro-mechanical voltage-speed link ($v_{d,q} - U$);
- the definition of magnetic flux linkage ($\Psi_{d,q}$);
- the electromagnetic thrust-current relation ($T_{em} - i_{d,q}$);
- the mechanical dynamic model

$$\begin{cases} \begin{bmatrix} v_d \\ v_q \end{bmatrix} = R_s \begin{bmatrix} i_d \\ i_q \end{bmatrix} + \dfrac{d}{dt} \begin{bmatrix} \Psi_d \\ \Psi_q \end{bmatrix} + \dfrac{\pi}{\tau} U \begin{bmatrix} -\Psi_q \\ \Psi_d \end{bmatrix} \\ \begin{bmatrix} \Psi_d \\ \Psi_q \end{bmatrix} = \begin{bmatrix} L_d & 0 \\ 0 & L_q \end{bmatrix} \begin{bmatrix} i_d \\ i_q \end{bmatrix} + \begin{bmatrix} \Phi_{PM} \\ 0 \end{bmatrix} \\ T_{em} = \dfrac{P_{em}}{U} = \dfrac{3}{2} \dfrac{\pi}{\tau} i_q \Big(\Phi_{PM} + (L_d - L_q) i_d \Big) \\ T_{em} = m \dfrac{dU}{dt} + B \cdot U + T_L + T_{cogging} \end{cases} \tag{A.1}$$

In Eq.A.1, R_s and $L_{d,q}$ represent the resistive and inductive components of the stator coil impedances in the dq domain equivalent circuits, Φ_{PM} the contribution of permanent magnets

to the total flux linkage, while U, m, B represent the mover speed, mass and viscous friction coefficient, respectively. In the last equation, the opposing thrust actually consists of two contributions: the actual load thrust T_L exerted by the mechanical load, and the cogging thrust $T_{cogging}$ related to parasitic magnetic co-energy [77].

A.2 Generation of reference currents

The third equation of Eq.A.1 shows that a set of two currents i_d and i_q is required to generate a specific electromagnetic thrust. As such, to produce a desired $T_{em,ref}$, an additional condition must be defined to retrieve a unique solution. Many techniques [77] exist to determine the couple of reference currents for the PI regulators, such as the $i_d = 0$ technique, the *Maximum Thrust Per Ampere* [80] (MTPA), and the *Field Weakening Control* [72]. Given the approximately unitary saliency ratio L_d/L_q, associated to the minimal contribution of the reluctance thrust with respect to the magnetic thrust, the simple $i_d = 0$ technique also coincides with the *MTPA*. From Eq.A.1, the generated reference currents are computed as:

$$\begin{cases} i_d = 0 \\ i_q = \dfrac{T_{em}}{\frac{3}{2}\frac{\pi}{\tau}\Phi} \end{cases} \tag{A.2}$$

The *MTPA* block, then, collapses into a simple gain block.

The reference currents are then transferred to the *constraints check* block to verify if current and voltage constraints are met. The choice of the coils wire section (AWG 26) imposes a maximum current capability of around 1.3 A for a 60 °C temperature rating insulator[1]. Actually, there is no unique guideline for the determination of the current capacity, which strongly depends on the ambient temperature and type of wiring.

From the maximum current condition, and considering the maximum average line-to-line voltage that the converter can apply (48 V) and the internal resistances of each phase coil (8.9 Ω), it is possible to estimate the maximum phase back-emf which V_{max} would induce the maximum current as:

$$V_{max} \approx \frac{V_{batt} + 2R_s I_{max}}{\sqrt{3}} \approx 41.1\,\mathrm{V}\,. \tag{A.3}$$

From this value, the maximum instantaneous speed U_{max} can be approximately derived as:

$$U_{max} \approx \frac{V_{max}}{\frac{\pi}{\tau}\Phi_{PM}} \approx 0.784\,\mathrm{m/s}\,. \tag{A.4}$$

According to Eq.A.5, the current and voltage limits can be graphically represented in a $i_{d,ref} - i_{q,ref}$ plane as a circumference and a speed-dependent ellipse, respectively ([80]). The working points determined by the *MTPA* block lie on the vertical axis (since $i_{d,ref} = 0$).

$$\begin{cases} \sqrt{i_d^2 + i_q^2} \leq I_{max} \\ \sqrt{\left(\dfrac{\pi}{\tau} U L_q i_q\right)^2 + \left[\dfrac{\pi}{\tau} U (L_d i_d + \Phi)\right]^2} \leq V_{max} \end{cases} \tag{A.5}$$

[1] https://en.wikipedia.org/wiki/American_wire_gauge#cite_note-small_gauge_ampacity-13

The working points belonging to the intersection of the two curve areas satisfy both the limits; if they don't, the *constraint check* block reduces the i_d current to reduce the d-axis flux linkage, in turns decreasing the d-axis back-emf until the allowed working region.

Fig.A.1 shows the current limit circle and two voltage limit ellipses (only partially visible) for the base speed (speed at which the maximum torque can be achieved at rated current and voltage conditions) and the maximum allowed speed for which a solution exists satisfying both current and voltage limits. Below the base speed, the *MTPA* algorithm always provides a solution satisfying the voltage limit. Above the base speed, the *MTPA* scheme does not meet the voltage limit requirement: suitably designed Look-Up Tables (LUTs) have been analytically designed to shift the working point along the intersection between the circumference and ellipse perimeters.

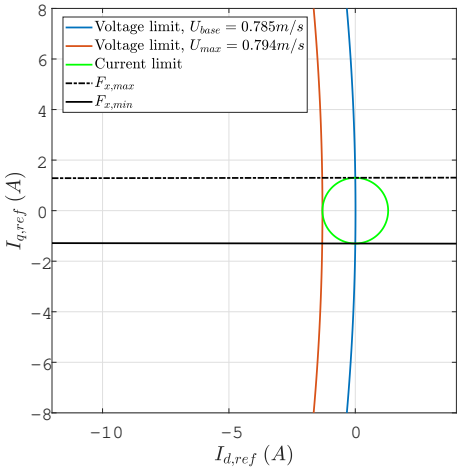

Figure A.1: Graphical representation of current and voltage limits in the $i_{d,ref} - i_{q,ref}$ plane.

A.3 Design of PI controllers

As mentioned in Chap.4, the PI controllers aim at regulating the phase currents to follow the reference currents generated by the external loop of the control system. Two PI controllers are designed in this work, for the d-axis and q-axis currents, respectively, even though the design provides very similar results. For the derivation of the current transfer function, it is assumed that the power converter is characterized by a first-order dynamic response linked to the switching period T_{sw}:

$$G_{inv}(s) = \frac{1}{1 + sT_{sw}} \,. \tag{A.6}$$

From the simplified block diagram in Fig.4.15, the current transfer functions become:

$$\frac{i_{dq}}{i_{ref,dq}} = \frac{sK_{p,dq} + K_{i,dq}}{s^3 L_{dq} T_{sw} + s^2(L_{dq} + R_s T_{sw}) + s(R_s + K_{p,dq}) + K_{i,dq}} \,. \tag{A.7}$$

By setting a reasonably low bandwidth, it is reasonable to neglect the 3^{rd} order term in the denominator to obtain a 2^{nd} order transfer function in the form:

$$H(s) = \frac{\omega_0^2}{s^2 + 2\xi\omega_0 s + \omega_0^2} \,, \tag{A.8}$$

where ω_0 is the natural frequency and ξ the damping factor of the dynamic response. This expression allows to derive explicit expressions for $K_{p,dq}$ and $K_{i,dq}$. The integral coefficient for each controller is designed by setting the desired bandwidth f_{BW} at 500 Hz, far enough from the switching frequency to filter out the switching noise:

$$K_{i,dq} \stackrel{!}{=} \omega_{BW}^2 (L_{dq} + R_s T_{sw}) \approx 20 \cdot 10^3 \Omega/s \,. \tag{A.9}$$

The proportional coefficients $K_{p,dq}$ are set to achieve a 10% maximum allowed overshoot (design equations in [81]):

$$K_{p,dq} \stackrel{!}{=} 2\xi\omega_{BW}(L_{dq} + R_s T_{sw}) - R_s \approx 10\Omega \,. \tag{A.10}$$

The ad-hoc PI controllers designed for this application exhibit the additional following features:

- a feedforward compensation of the back-emf for both the d-axis and q-axis, to increase the responsiveness of the control;
- an integral clamping anti-windup scheme, to block the integral action when the output control voltage is saturated to V_{max}, and preventing the accumulation of errors. In this way, the recovery from saturation (open loop control condition) is faster.

Fig.A.2 displays the adopted Simulink model for the PI controllers endowed with feedforward compensation and ad-hoc integral clamping anti-windup networks.

Actually, the here presented design in continuous domain is then discretised to be uploaded on the control board.

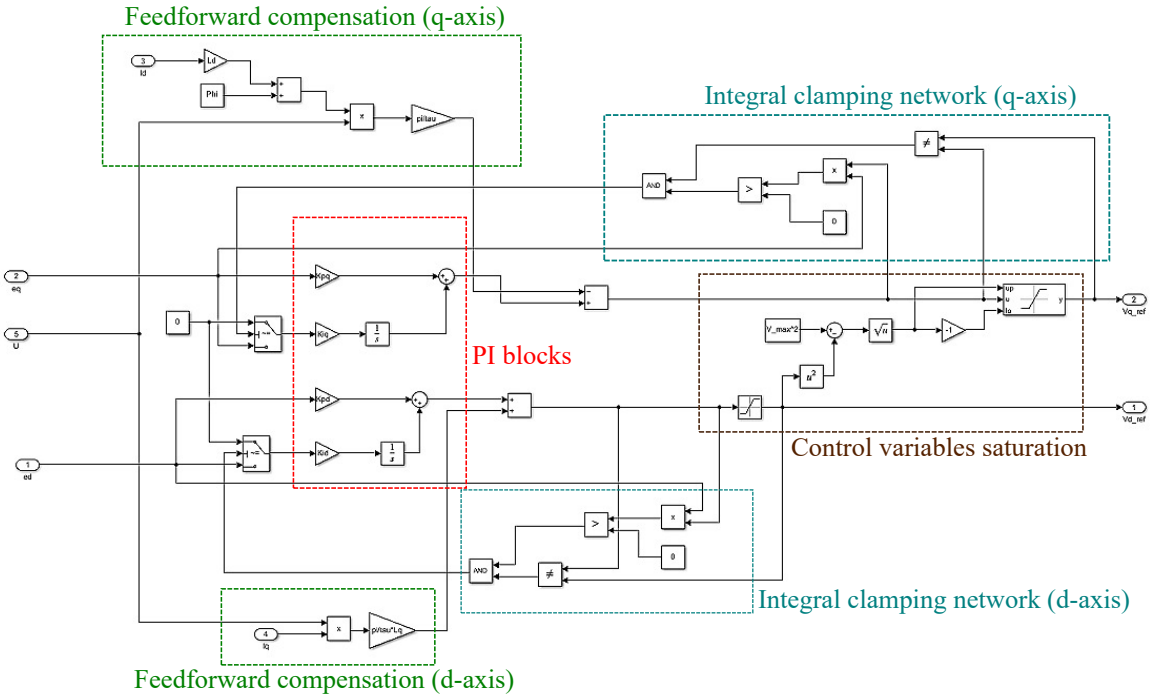

Figure A.2: Simulink model of the designed PI controllers.

Appendix B

Team organization and Gantt chart

The multidisciplinary project, key element for the Alta Scuola Politecnica curricular path, required the integration of diversified backgrounds. In general, the team worked in two parallel, but communicating, subgroups, dealing with the Multiphysics design of the regenerator and the Power Electronics converter and control, respectively. Full Professor Giovanni Maizza and research Engineer Umid Jamolov (Politecnico di Torino) provided guidance and support to the first group in the use of the *Comsol Multiphysics* software and through the design process of the damper. They also mediated between the team activities and Frandent Group, to set short- and mid-term deadlines. Associate Professor Luigi Piegari (Politecnico di Milano) supported the second subgroup in the acquisition of background knowledge on electrical machines and assisted through the control design phase.

The two subgroups arrange their weekly work independently for most of the duration of the project. During the last months, it was instead necessary a combined approach for the extraction of the electrical model of the damper (link between the multiphysical design and the control design), and for the testing phase. The contribution of each component is here listed.

Omar Kahol (Aeronautical Engineering, PoliMi), specialized in fluidodynamics and computational mechanics, contributed to the literature review of damping systems applied to automotive and aerospace fields, and road excitation and car modelling. During the Multiphysics design phase, he gave is contribution in the parallel studying of linear and rotary machines, and designed the simulation setup to extract the parametres of the electrical circuit model, needed for the control design.

Lorenzo Mai (Engineering Physics, PoliMi), specialized in physics of matter and light phenomena, outlined the current state of the art of electromagnetic dampers, with specific focus on the magnets array configuration and the materials for the various parts of the damper. He guided the geometrical parametres tuning and material selection on the basis of the minimization of losses linked to magnetic hysteresis and Eddy currents.

Andrea Proietti (Mechatronics Engineering, PoliTo), with a combined background in mechanical and control engineering, worked as well in the Multiphysics subgroup, specifically in the iterative tuning process of the geometrical parametres of the damper and coils. His background in control engineering was also helpful in the definition and validation of the electronic control model, and in the generation of processor-in-the-loop (PIL) simulation tests.

Stefano Cerutti (Electronic Engineering, PoliTo), specialized in power electronics, worked in the second subgroup. He worked on the literature review of rotary and linear machines, specifically from the point of view of electrical modelling and control techniques, and applied this knowledge in the analytic design of the control system. He helped in the electronic components selection and purchase, and coordinated the laboratory activities with the academic tutors.

Tan Tran Duc (Electronic Engineering, PoliTo), specialized in micro- and nano-electronics, worked on the literature review of energy harvesting systems, and contributed to the electronic control design. His background in digital electronics was helpful in the hardware programming (evaluation board) and in the characterization of sensors.

Francesca Stobbione (Industrial Production and Innovation Technology Engineering, PoliTo), coordinated the two subgroups at a higher level, managing the communication with academic

tutors and the ASP board, and helping defining deadlines and sub-tasks. In a first phase, she investigated the stakeholders' environment around REGIM, also through direct contacts with Frandent. She managed the budget use and the purchase of components for the laboratory testing.

Fig.B.1 reports the definitive Gantt chart of the project activities, subdivided by team and type (research, design, procurement/testing, and data analysis/documentation). As described, the activities of the two groups proceeded in parallel during the literature review phase and the design phase (beside the definition of specifications, concerning the entire group). The experimental phase involved both the subgroups in both organization and testing.

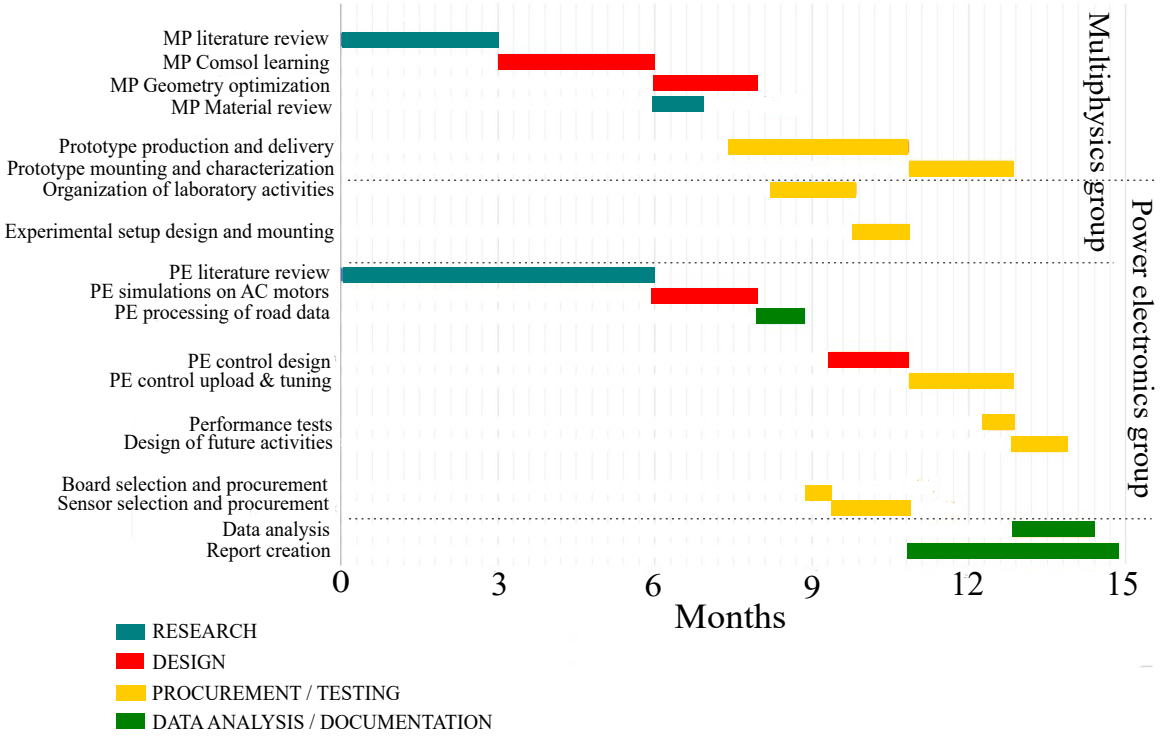

Figure B.1: Gantt chart of the team activities.

Bibliography

[1] J. W. Erisman, M. A. Sutton, J. Galloway, Z. Klimont, and W. Winiwarter, "How a century of ammonia synthesis changed the world," *Nature Geoscience*, vol. 1, pp. 636–639, Sept. 2008.

[2] FAO, "Sustainable agricultural mechanization." Available at: https://www.fao.org/sustainable-agricultural-mechanization/overview/why-mechanization-is-important/en/, 2022. Accessed: August 2022.

[3] J. Sachs, C. Kroll, G. Lafortune, G. Fuller, and F. Woelm, *Sustainable Development Report 2022*. Cambridge University Press, 2022.

[4] R. Zhang, X. Wang, and S. John, "A comprehensive review of the techniques on regenerative shock absorber systems," *Energies*, vol. 11, no. 5, 2018.

[5] B. Lafarge, S. Cagin, O. Curea, and A. Perret, "From functional analysis to energy harvesting system design: application to car suspension," *International Journal on Interactive Design and Manufacturing (IJIDeM)*, vol. 10, pp. 37–50, 2014.

[6] R. Oprea, M. Mihailescu, A. I. Chirila, and I. Deaconu, "Design and efficiency of linear electromagnetic shock absorbers," *2012 13th International Conference on Optimization of Electrical and Electronic Equipment (OPTIM)*, pp. 630–634, 2012.

[7] L. Zuo, B. Scully, J. Shestani, and Y. Zhou, "Design and characterization of an electromagnetic energy harvester for vehicle suspensions," *Smart Materials and Structures*, vol. 19, p. 045003, feb 2010.

[8] J. Rockström, W. Steffen, K. Noone, Å. Persson, F. S. Chapin, E. F. Lambin, T. M. Lenton, M. Scheffer, C. Folke, H. J. Schellnhuber, B. Nykvist, C. A. de Wit, T. Hughes, S. van der Leeuw, H. Rodhe, S. Sörlin, P. K. Snyder, R. Costanza, U. Svedin, M. Falkenmark, L. Karlberg, R. W. Corell, V. J. Fabry, J. Hansen, B. Walker, D. Liverman, K. Richardson, P. Crutzen, and J. A. Foley, "A safe operating space for humanity," *Nature*, vol. 461, pp. 472–475, Sept. 2009.

[9] F. G. SRL, "Frandent | azienda." Available at: https://www.frandent.it/it/azienda, 2022. Accessed: April 2022.

[10] U. Jamolov and G. Maizza, "Integral methodology for the multiphysics design of an automotive eddy current damper," *Energies*, vol. 15, no. 3, 2022.

[11] W. FuJun, Y. Zhou, O. YingGang, Z. XiangJun, and D. JieLi, ""government-industry-university-research- promotion" collaborative innovation mechanism construction to promote the development of agricultural machinery technology," *IFAC-PapersOnLine*, vol. 51, no. 17, pp. 552–559, 2018.

[12] E. J. Mantoam, G. Angnes, M. M. Mekonnen, and T. L. Romanelli, "Energy, carbon and water footprints on agricultural machinery," *Biosystems Engineering*, vol. 198, pp. 304–322, Oct. 2020.

[13] M. Varani, M. Mattetti, and G. Molari, "Performance evaluation of electrically driven agricultural implements powered by an external generator," *Agronomy*, vol. 11, no. 8, 2021.

[14] D. Bowers, "Farm power and mechanization for small farms in sub-saharan africa. by b. g. sims and j. kienzle. rome: Food and agriculture organization of the united nations (2006), pp. 65, us$26.00. issn 1814-1137," *Experimental Agriculture - EXP AGR*, vol. 43, 07 2007.

[15] "Global market study on automotive shock absorbers: Increasing vehicle production and parc to aid demand growth over coming years." Available at:

https://www.persistencemarketresearch.com/market-research/shock-absorbers-market.asp, 2021. Accessed: July 2022.

[16] R. Schnepf, "Energy use in agriculture: Background and issues," *University of North Texas Libraries*, 11 2004.

[17] B. Lafarge, S. Grondel, C. Delebarre, O. Curea, and C. Richard, "Linear electromagnetic energy harvester system embedded on a vehicle suspension: From modeling to performance analysis," *Energy*, vol. 225, p. 119991, 2021.

[18] R. Galluzzi, S. Circosta, N. Amati, and A. Tonoli, "Rotary regenerative shock absorbers for automotive suspensions," *Mechatronics*, vol. 77, p. 102580, 2021.

[19] N. Amati, A. Festini, and A. Tonoli, "Design of electromagnetic shock absorbers for automotive suspensions," *Vehicle System Dynamics*, vol. 49, no. 12, pp. 1913–1928, 2011.

[20] U. Aksu and R. Halicioglu, "A review study on energy harvesting systems for vehicles," *Tehnički glasnik*, vol. 12, no. 4, pp. 251–259, 2018.

[21] D. Chandler, "More power from bumps in the road," *MIT Tech Talk*, vol. 53, no. 15, p. 4, 2009.

[22] L. Cannizzaro, G. V. Mariotti, A. Giallanza, G. Marannano, G. V. Mariotti, and M. Porretto, "Design of an electromagnetic regenerative damper and energy harvesting assessment," 2016.

[23] J. Zhang, H. Yu, Q. Chen, M. Hu, L. Huang, and Q. Liu, "Design and experimental analysis of ac linear generator with halbach pm arrays for direct-drive wave energy conversion," *IEEE Transactions on Applied Superconductivity*, vol. 24, no. 3, pp. 1–4, 2014.

[24] B. Drew, A. R. Plummer, and M. N. Sahinkaya, "A review of wave energy converter technology," 2009.

[25] G. C. Conroy and P. Sideris, "Exploring energy harvesting and vibration mitigation in tall buildings accounting for wind and seismic loads," *Engineering Structures*, vol. 247, p. 113126, 2021.

[26] F. Mazza and A. Vulcano, "Control of the earthquake and wind dynamic response of steel-framed buildings by using additional braces and/or viscoelastic dampers," *Earthquake Engineering & Structural Dynamics*, vol. 40, no. 2, pp. 155–174, 2011.

[27] H. Lee, H. Jang, J. Park, S. Jeong, T. Park, and S. Choi, "Design of a Piezoelectric Energy-Harvesting Shock Absorber System for a Vehicle," *Integrated Ferroelectrics*, vol. 141, pp. 32–44, Jan. 2013. Publisher: Taylor & Francis _eprint: https://doi.org/10.1080/10584587.2013.778724.

[28] X. D. Xie and Q. Wang, "Energy harvesting from a vehicle suspension system," *Energy*, vol. 86, pp. 385–392, June 2015.

[29] S. Priya, "Advances in energy harvesting using low profile piezoelectric transducers," *Journal of Electroceramics*, vol. 19, pp. 167–184, Sept. 2007.

[30] I. C. Lien and Y. C. Shu, "Array of piezoelectric energy harvesting by the equivalent impedance approach," *Smart Materials and Structures*, vol. 21, p. 082001, July 2012. Publisher: IOP Publishing.

[31] P. D. Mitcheson, E. K. Reilly, P. K. Wright, and E. H. Yeatman, "Transduction Mechanisms and Power Density for MEMS Inertial Energy Scavengers," in *Proceedings of Power MEMS 06, Berkeley, USA*, Nov. 2006. Accepted: 2009-08-18T10:58:21Z.

[32] H. S. Corp, "Regenerative damping method and apparatus (expired)," no. US6920951B2, 2003.

[33] A. Tonoli, "Dynamic characteristics of eddy current dampers and couplers," *Journal of Sound and Vibration*, vol. 301, no. 3, pp. 576–591, 2007.

[34] S. Zhu, W.-A. Shen, and Y.-L. Xu, "Linear electromagnetic devices for vibration damping and energy harvesting: Modeling and testing," *Eng. Struct.*, vol. 34, pp. 198–212, Jan. 2012.

[35] H. Chen, S. Zhao, H. Wang, and R. Nie, "A novel single-phase tubular permanent magnet linear generator," *IEEE Transactions on Applied Superconductivity*, vol. 30, no. 4, pp. 1–5, 2020.

[36] J. P. A. Bastos and N. Sadowski, *Magnetic Materials and 3D Finite Element Modeling*. CRC Press, Apr. 2017.

[37] A. Talaat, M. Suraj, K. Byerly, A. Wang, Y. Wang, J. Lee, and P. Ohodnicki, "Review on soft magnetic metal and inorganic oxide nanocomposites for power applications," *Journal of Alloys and Compounds*, vol. 870, p. 159500, 2021.

[38] F. Fiorillo, G. Bertotti, C. Appino, and M. Pasquale, "Soft magnetic materials."

[39] T. Kasagi, T. Tsutaoka, and K. Hatakeyama, "Electromagnetic properties of permendur granular composite materials containing flaky particles," *Journal of Applied Physics*, vol. 116, no. 15, p. 153901, 2014.

[40] K. Chwastek, J. SzczygŁowski, and W. Wilczyński, "Modelling magnetic properties of high silicon steel," *Journal of Magnetism and Magnetic Materials*, vol. 322, pp. 799–803, 2010.

[41] G. Ouyang, X. Chen, Y. Liang, C. Macziewski, and J. Cui, "Review of fe-6.5wt%si high silicon steel—a promising soft magnetic material for sub-khz application," *Journal of Magnetism and Magnetic Materials*, vol. 481, pp. 234–250, 2019.

[42] K. Takenaka, A. D. H. Setyawan, P. Sharma, N. Nishiyama, and A. Makino, "Industrialization of nanocrystalline fe–si–b–p–cu alloys for high magnetic flux density cores," *Journal of Magnetism and Magnetic Materials*, vol. 401, pp. 479–483, 2016.

[43] N. Nishiyama, K. Tanimoto, and A. Makino, "Outstanding efficiency in energy conversion for electric motors constructed by nanocrystalline soft magnetic alloy "nanomet®" cores," *AIP Advances*, vol. 6, p. 055925, 2016.

[44] K. Suzuki, R. Parsons, B. Zang, K. Onodera, H. Kishimoto, and A. Kato, "Copper-free nanocrystalline soft magnetic materials with high saturation magnetization comparable to that of si steel," *Applied Physics Letters*, vol. 110, no. 1, p. 012407, 2017.

[45] T. Takahashi, K. Yoshida, Y. Shimizu, A. Setyawan, M. Bito, M. Abe, and A. Makino, "Fe-si-b-p-c-cu nanocrystalline soft magnetic powders with high b s and low core loss," *AIP Advances*, vol. 7, p. 056111, 05 2017.

[46] R. Wang, R. Ding, and L. Chen, "Application of hybrid electromagnetic suspension in vibration energy regeneration and active control," *Journal of Vibration and Control*, vol. 24, pp. 223–233, Jan. 2018. Publisher: SAGE Publications Ltd STM.

[47] S. Dwari and L. Parsa, "An Efficient AC–DC Step-Up Converter for Low-Voltage Energy Harvesting," *IEEE Transactions on Power Electronics*, vol. 25, pp. 2188–2199, Aug. 2010. Conference Name: IEEE Transactions on Power Electronics.

[48] R. Dayal, S. Dwari, and L. Parsa, "Design and Implementation of a Direct AC–DC Boost Converter for Low-Voltage Energy Harvesting," *IEEE Transactions on Industrial Electronics*, vol. 58, pp. 2387–2396, June 2011. Conference Name: IEEE Transactions on Industrial Electronics.

[49] E. Arroyo and A. Badel, "Electromagnetic vibration energy harvesting device optimization by synchronous energy extraction," *Sensors and Actuators A: Physical*, vol. 171, pp. 266–273, Nov. 2011.

[50] C.-Y. Hsieh, *Energy harvesting and control of a regenerative suspension system using switched mode converters*. Thesis, Applied Sciences:, Dec. 2014.

[51] L. Xie, J. Li, X. Li, L. Huang, and S. Cai, "Damping-tunable energy-harvesting vehicle damper with multiple controlled generators: Design, modeling and experiments," *Mechanical Systems and Signal Processing*, vol. 99, pp. 859–872, Jan. 2018.

[52] Y. M. Roshan, A. Maravandi, and M. Moallem, "Power Electronics Control of an Energy Regenerative Mechatronic Damper," *IEEE Transactions on Industrial Electronics*, vol. 62,

pp. 3052–3060, May 2015. Conference Name: IEEE Transactions on Industrial Electronics.

[53] S.-Y. Jung and K. Nam, "Pmsm control based on edge-field hall sensor signals through anf-pll processing," *IEEE Transactions on Industrial Electronics*, vol. 58, no. 11, pp. 5121–5129, 2011.

[54] M. A. M. Cheema, J. E. Fletcher, M. F. Rahman, and D. Xiao, "Optimal, combined speed, and direct thrust control of linear permanent magnet synchronous motors," *IEEE Transactions on Energy Conversion*, vol. 31, no. 3, pp. 947–958, 2016.

[55] L. J.P., *Control of Synchronous Motors*. Wiley, 2011.

[56] L. Yongdong and Z. Hao, "Sensorless control of permanent magnet synchronous motor — a survey," in *2008 IEEE Vehicle Power and Propulsion Conference*, pp. 1–8, 2008.

[57] A. Qiu, B. Wu, and H. Kojori, "Sensorless control of permanent magnet synchronous motor using extended kalman filter," in *Canadian Conference on Electrical and Computer Engineering 2004 (IEEE Cat. No.04CH37513)*, vol. 3, pp. 1557–1562 Vol.3, 2004.

[58] Y.-S. Han, J.-S. Choi, and Y.-S. Kim, "Sensorless pmsm drive with a sliding mode control based adaptive speed and stator resistance estimator," *IEEE Transactions on Magnetics*, vol. 36, no. 5, pp. 3588–3591, 2000.

[59] ISO, Geneva, Switzerland, "Mechanical vibration — Road surface profiles — Reporting of measured data," 2016.

[60] M. Agostinacchio, D. Ciampa, and S. Olita, "The vibrations induced by surface irregularities in road pavements – a matlab® approach," *Eur. Transp. Res. Rev.*, vol. 6, pp. 267–275, Sept. 2014.

[61] A. Chamseddine, H. Noura, and T. Raharijaona, "Full vehicle active suspension: Sensor fault diagnosis and fault tolerance," in *Fault Detection, Supervision and Safety of Technical Processes 2006*, pp. 468–473, Elsevier, 2007.

[62] W. Gao, N. Zhang, and J. Dai, "A stochastic quarter-car model for dynamic analysis of vehicles with uncertain parameters," *Vehicle System Dynamics*, vol. 46, no. 12, pp. 1159–1169, 2008.

[63] B. Lafarge, S. Grondel, C. Delebarre, O. Curea, and C. Richard, "Linear electromagnetic energy harvester system embedded on a vehicle suspension: From modeling to performance analysis," *Energy*, vol. 225, p. 119991, 2021.

[64] J. Subramanian, D. P. Famouri, F. Mahmudzadeh, and M. Bade, "Comparison of halbach, radial and axial magnet arrangement for single phase tubular permanent magnet linear alternators," in *2020 IEEE Electric Power and Energy Conference (EPEC)*, pp. 1–5, 2020.

[65] J. Moermond, "Magnetic field sensors - are magnets different?." *Automation Insights*, Available at: https://automation-insights.blog/2010/04/26/magnetic-field-sensors-, Jun 2010. Accessed: August 2022.

[66] R. K. Sharma, V. Sanadhya, L. Behera, and S. Bhattacharya, "Vector control of a permanent magnet synchronous motor," in *2008 Annual IEEE India Conference*, vol. 1, pp. 81–86, 2008.

[67] V. Rallabandi, N. Taran, D. M. Ionel, and P. Zhou, "Inductance testing for ipm synchronous machines according to the new ieee std 1812 and typical laboratory practices," *IEEE Transactions on Industry Applications*, vol. 55, no. 3, pp. 2649–2659, 2019.

[68] L. S. Maraaba, Z. M. Al-Hamouz, A. S. Milhem, and S. Twaha, "Comprehensive parameters identification and dynamic model validation of interior-mount line-start permanent magnet synchronous motors," *Machines*, vol. 7, no. 1, 2019.

[69] M. Haque and M. Rahman, "Dynamic model and parameter measurement of interior permanent magnet synchronous motor," 01 1999.

[70] I. Boldea and S. A. Nasar, *Electric Drives (2^{nd} Edition)*. CRC Press, 1998.

[71] X. Zhang, X. Xie, and R. Yao, "Field oriented control for permanent magnet synchronous

motor based on dsp experimental platform," in *The 27th Chinese Control and Decision Conference (2015 CCDC)*, pp. 1870–1875, 2015.

[72] K. Zhou, M. Ai, D. Sun, N. Jin, and X. Wu, "Field weakening operation control strategies of pmsm based on feedback linearization," *Energies*, vol. 12, p. 4526, 11 2019.

[73] X. Liu, H. Chen, J. Zhao, and A. Belahcen, "Research on the performances and parameters of interior pmsm used for electric vehicles," *IEEE Transactions on Industrial Electronics*, vol. 63, no. 6, pp. 3533–3545, 2016.

[74] M. Saetti, M. Mattetti, M. Varani, N. Lenzini, and G. Molari, "On the power demands of accessories on an agricultural tractor," *Biosystems Engineering*, vol. 206, pp. 109–122, 2021.

[75] FAOSTAT, "Emissions shares." Available at: https://www.fao.org/faostat/en/data/EM/visualize, 2021. Accessed: June 2022.

[76] T. Rudnicki, R. Czerwinski, D. Polok, and A. Sikora, "Performance analysis of a pmsm drive with torque and speed control," in *2015 22nd International Conference Mixed Design of Integrated Circuits Systems (MIXDES)*, pp. 562–566, 2015.

[77] I. Boldea, *Linear Electric Machines, Drives, and MAGLEVs Handbook*. CRC Press, 2017.

[78] I. Boldea and S. A. Nasar, "Permanent-magnet linear alternators part 1: Fundamental equations," *IEEE Transactions on Aerospace and Electronic Systems*, vol. AES-23, no. 1, pp. 73–78, 1987.

[79] Z. Deng, I. Boldea, and S. Nasar, "Forces and parameters of permanent magnet linear synchronous machines," *IEEE Transactions on Magnetics*, vol. 23, no. 1, pp. 305–309, 1987.

[80] M. Caruso, A. Di Tommaso, M. Lombardo, R. Miceli, C. Nevoloso, and C. Spataro, "Maximum torque per ampere control algorithm for low saliency ratio interior permanent magnet synchronous motors," in *2017 IEEE 6th International Conference on Renewable Energy Research and Applications (ICRERA)*, pp. 1186–1191, 2017.

[81] K. Odo, E. Sochima Vincent, and C. Ogbuka, "A model-based pi controller tuning and design for field oriented current control of permanent magnet synchronous motor," *IOSR Journal of Electrical and Electronics Engineering (IOSR-JEEE)*, vol. 14, pp. 35–41, 08 2019.